New Journal of Physics
The open access journal at the forefront of physics

Deutsche Physikalische Gesellschaft DPG IOP Institute of Physics

PAPER • OPEN ACCESS

What defines the quantum regime of the free-electron laser?

To cite this article: Peter Kling *et al* 2015 *New J. Phys.* **17** 123019

New Journal of Physics
The open access journal at the forefront of physics

Deutsche Physikalische Gesellschaft DPG
IOP Institute of Physics

Published in partnership with: Deutsche Physikalische Gesellschaft and the Institute of Physics

OPEN ACCESS

RECEIVED
5 August 2015

REVISED
30 September 2015

ACCEPTED FOR PUBLICATION
15 October 2015

PUBLISHED
14 December 2015

PAPER

What defines the quantum regime of the free-electron laser?

Peter Kling[1,2,4], **Enno Giese**[2,4], **Rainer Endrich**[1,2], **Paul Preiss**[1,2], **Roland Sauerbrey**[1] **and Wolfgang P Schleich**[2,3]

[1] Helmholtz-Zentrum Dresden-Rossendorf eV, D-01328 Dresden, Germany
[2] Institut für Quantenphysik and Center for Integrated Quantum Science and Technology (IQ^{ST}), Universität Ulm, Albert-Einstein-Allee 11, D-89081, Germany
[3] Texas A&M University Institute for Advanced Study (TIAS), Institute for Quantum Science and Engineering (IQSE), and Department of Physics and Astronomy, Texas A&M University, College Station, TX 77843-4242, USA
[4] These authors contributed equally.

E-mail: peter.kling@uni-ulm.de

Keywords: free-electron laser, quantum regime, Quantum FEL

Abstract

The quantum regime of the free-electron laser (FEL) emerges when the discreteness of the momentum of the electron plays a dominant role in the interaction with the laser and the wiggler field. Motivated by a heuristic phase space approach we pursue two different routes to define the transition from the classical FEL to the quantum domain: (i) standard perturbation theory and (ii) the method of averaging. Moreover, we discuss the experimental requirements for realizing a Quantum FEL and connect them to today's capabilities.

1. Introduction

For all free-electron lasers (FELs) presently in operation a description within classical electrodynamics suffices. However, there exists a regime where quantum mechanics plays a central role. Based on a description within a co-moving frame of reference, where a single electron interacts with a quantized standing light field, we propose a definition of and formulate the conditions for this quantum regime. Depending on the value of a single parameter the electron dynamics reduces from an infinite ladder of momenta to a two-level behavior. To bring this two-level nature to light we use the powerful asymptotic method of averaging over fast oscillations.

1.1. What is a Quantum FEL?

In complete analogy to Compton scattering the microscopic mechanisms of an FEL [1] can easily be understood as two subsequent scattering processes: the electron annihilates a photon of the wiggler field and decelerates by the amount of the photon momentum; then the electron scatters a photon into the copropagating laser field and loses again momentum, which corresponds to the momentum of the laser photon. Thus, the change of momentum caused by such a scattering process is always given by a fixed value of the recoil, leading to discrete steps for the electron momentum. This statement is also true for the inverse process when a laser photon is annihilated and a wiggler photon is created. However, for all existing FELs this discrete quantum mechanical recoil is of minor importance and the electrons follow classical trajectories [2–4].

The current development of FELs focuses on the X-ray regime of radiation as exemplified by the LCLS at SLAC in Stanford [5] or the European XFEL at DESY in Hamburg [6]. With decreasing wavelengths, the quantum mechanical recoil which is proportional to the wave number of the laser field increases and the emergence of a domain where the discreteness of the momentum does play a role for the FEL dynamics is evident. This new regime of FEL-operation, the so-called quantum regime or Quantum FEL, was theoretically predicted by Bonifacio *et al* [7]. It is expected that a Quantum FEL displays better radiation properties such as a narrower linewidth and better temporal coherence in comparison to its classical counterpart [8]. Even though an experimental realization is still far from reach, due to progress in the fields of accelerator and laser physics it might be possible within the future.

The goal of our article is to define a Quantum FEL and analyze the conditions under which it can be realized. The full dynamics of an FEL is given by an infinite ladder of momenta which form a continuum in the classical limit. The opposite is the case in the quantum regime: the discreteness of the momentum states of the electron becomes crucial. Moreover, by going deeper into the quantum regime we can reduce the number of relevant momentum states until we reach an effective two-level system. We emphasize that a theory based on classical physics is not applicable in this limit since we do not deal with continous trajectories but with discrete momentum steps which makes a quantum theory mandatory.

1.2. Connection to existing literature

It is interesting to note that the first theories of an FEL were based on quantum mechanics [9] before it became evident that classical physics suffices for most of the situations [2, 3, 10]. However, also after this important insight there was still interest in developing a quantum description for the FEL, which was e.g. done in [11] by using perturbation theory to calculate the gain of the laser field. It was soon recognized [12] that this procedure was not applicable to a classical device where thousands of photons are emitted by a single electron [13]. Perturbation theory only 'accidently' gives the correct results and there was a need for more sophisticated approaches [12, 14, 15].

The main interests of these theories lie on the one hand in the explanation of the *classical regime* of FEL dynamics and on the other hand in the calculation of genuine quantum features of the radiation such as the photon statistics and the natural linewidth [16–18]. A *quantum regime* as proposed in our article was of minor importance.

However, the interest in this regime rose during the first years of the new millenium [7, 19]: in a many-electron theory the collective variables, introduced in [20], were quantized in a symmetrized way and the Heisenberg equations for these operators were linearized in the short-time limit [21]. In the resulting characteristic equation one found quantum corrections to the classical case and could identify the Quantum FEL as the limit when these corrections, quantified by a quantum parameter, become dominant. From the resulting dynamics the effective two-level behavior was deduced.

Our approach takes the opposite direction: starting from the full dynamics we directly *search* for the regime where the continuum of momenta reduce to two discrete levels. Using asymptotic methods we find the emergence of the quantum regime in a rigorous manner and can identify its origin in the occurence of two different time scales in the dynamical equations. The ratio of the two frequencies connected to these time scales defines *our* quantum parameter, which is the expansion parameter of our asymptotic series.

1.3. Our approach and summary of results

How can we destill the two-level behavior of the Quantum FEL from the full dynamics? In order to develop an intuitive model starting from first principles and introduce only the fundamental concepts of our approach, we restrict ourselves in this article to a single-electron and single-mode theory.

In an illustrative approach in phase space we first search for the limits of the classical description and the conditions for operating the FEL in a quantum regime. Already in this picture we can deduce the crucial quantity for the transition to the quantum regime, that is the quantum parameter α, which is the analogue of the quantum parameter of $\bar{\rho}$ of [21]. It is given by the ratio of the coupling between the electron and the fields and a frequency which is connected to the quantum mechanical recoil. Moreover, we realize that we additionally need a narrow initial momentum distribution for the electron to see the discreteness of the momenta.

However, we still have to develop a rigorous proof for the two-level behavior starting from a quantum mechanical description. The first method we use to achieve this goal is ordinary perturbation theory valid only for short times. We again find the quantum parameter α governing the transition to the quantum regime. For increasing values of the recoil this parameter becomes small and only single-photon processes are relevant since higher-order processes are suppressed. Furthermore, with the help of this method we recognize that the requirement on the width of the electron momentum distribution, mentioned above, is essential to obtain gain in the Quantum FEL.

Guided by the results of perturbation theory, we apply the method of averaging [22] which is more suitable for our situation. This technique brings out the transition to the two-level behavior most clearly. Similar to the rotating-wave approximation, well-known in the field of quantum optics [23], we average over rapid oscillations. These occur in the dynamical equations for the FEL when the quantum mechanical recoil becomes more and more prominent.

In lowest order of this asymptotic expansion only two momentum states are relevant and the dynamics is given by Rabi oscillations analogous to a two-level atom. This gives us the chance to make the connection of the Quantum FEL to the one-atom maser [23, 24]. Moreover, we can calculate the corrections to this deep quantum

regime which scale with powers of our quantum parameter. We find excellent agreement between these analytical expressions and numerical simulations.

We emphasize that our model covers only the most fundamental situation. Necessary extensions, i.e. a many-electron model and the inclusion of many modes of the radiation field are subject to future publications which, however, will be strongly influenced by the main ideas shown in the present article and in our recent publications [25].

1.4. Outline

Our article is organized as follows: we begin in section 2 with an intuitive discussion of the emergence of the quantum regime starting from a classical picture. Here, we introduce the quantum parameter α which characterizes this transition and obtain a condition for the width of the initial momentum distribution for the electron. We proceed in section 3 by recalling the basic elements of the quantum description of the FEL in a co-moving frame of reference, the so-called Bambini–Renieri frame [26]. In section 4 we then use conventional perturbation theory to find the conditions for the emergence of the quantum regime in the short-time limit. The results of this section serve us as a motivation to apply in section 5 the more sophisticated method of averaging [22] particularly suited for our problem. In this way we obtain the two-level behavior of the Quantum FEL even for longer times. Hence, we are in the position to connect our model to the Jaynes–Cummings [27] Hamiltonian, describing a two-level atom interacting with a quantized radiation field. In section 6 we rewrite the conditions for the emergence and operation of the Quantum FEL in a form which is more suitable for an experimental realization, before we summarize our main ideas and conclude in section 7.

To keep this article self-contained we recall in appendix A the transformation from the laboratory into the Bambini–Renieri frame and rederive in appendix B the Hamiltonian used throughout this article. In the appendices C and D we present the detailed calculations arising in the perturbative short-time limit and for the method of averaging, respectively.

2. Limits of the classical theory illuminated in phase space

The term 'Classical Laser' [10] at first sight seems paradox. However, the basic principles of lasers can be understood by classical physics, and the FEL is the prime example for such a classical laser [2, 3]. Nevertheless, electrons are quantum mechanical objects and on the microscopic level the change of the momentum of the electrons in the FEL is discrete, as already discussed in the introduction.

The momentum transfer from the photons to the electron is proportional to the wave number of the radiation. Hence, for decreasing wavelengths the quantum mechanical recoil increases and at some point dominates the dynamics of the FEL. In this domain the classical description of the electron-light interaction reaches its limit.

Starting from classical trajectories in phase space we now illustrate the conditions for which the discreteness of the recoil becomes essential and a quantum theory is mandatory. The illustrative model developed in this section serves us as a guide when we develop a rigorous quantum mechanical approach in the following sections.

2.1. Basic elements of the classical FEL theory

The classical low-gain FEL can be described by the one-dimensional Hamiltonian, equation (B.6),

$$H \equiv \frac{p^2}{2m} + V_0 \cos(2kz) \tag{1}$$

for a single electron with position z and its conjugate momentum p. This description is nonrelativistic, since we transformed from the laboratory frame into the co-moving Bambini–Renieri frame [26]. In this frame of reference, discussed in detail in appendix A, the wave numbers of the laser field k_{L} and the wiggler field k_{W} coincide, i.e. $k_{\mathrm{L}} = k_{\mathrm{W}} \equiv k$, and thus there is no explicit time-dependence in the Hamiltonian equation (1).

The potential height

$$V_0 \equiv 2\frac{e^2}{m} \left|\tilde{\mathcal{A}}_{\mathrm{L}}\right| \tilde{\mathcal{A}}_{\mathrm{W}} = 2\hbar g\sqrt{n} \tag{2}$$

is given by the product of the amplitudes of the vector potentials $\tilde{\mathcal{A}}_{\mathrm{L}}$ of the laser and the wiggler field $\tilde{\mathcal{A}}_{\mathrm{W}}$ with e being the elementary charge and m the mass of the electron.

Here we have neglected the change of the laser field during one pass of an electron with $\tilde{\mathcal{A}}_{\mathrm{L}} \approx \mathcal{A}_{\mathrm{L}}\sqrt{n} \approx$ const. In the second step we have introduced the reduced Planck constant $\hbar$ and have used the definition of g, equation (B.7), in order to make the connection to the quantum mechanical description in the later sections.

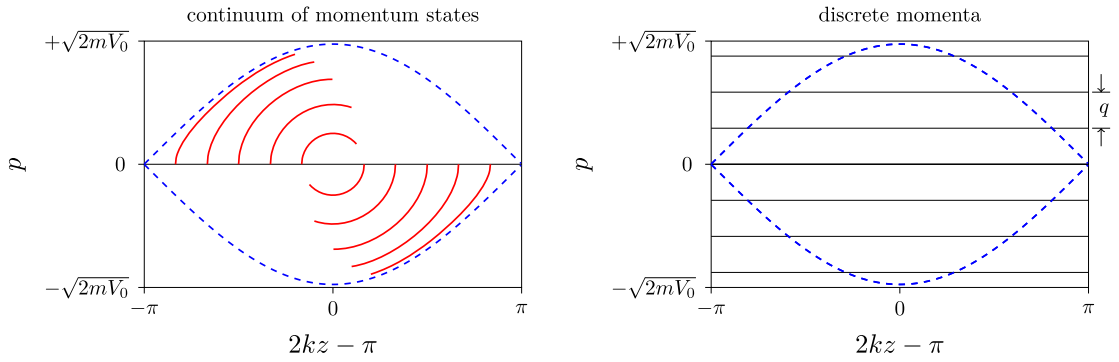

Figure 1. The FEL viewed from phase space (z,p) in the classical (left) and in the quantum regime (right). In the classical case the electrons follow continous trajectories (red lines), governed by the Hamiltonian equation (1). The dashed line indicates the separatrix defined by equation (3), which separates bounded and unbounded motion. The classical description loses its validity when the recoil $q = 2\hbar k$ is of the order of the maximal momentum $\pm\sqrt{2mV_0}$ as indicated by the horizontal lines representing the discrete momentum ladder displayed on the right-hand side.

A detailed discussion of the classical dynamics of the FEL can be found in [28]. In this section we briefly sketch the central idea in order to bring out most clearly the difference between the classical and the Quantum FEL.

The electron motion in phase space arising from equation (1) is shown on the left-hand side of figure 1. The electron undergoes a bounded motion if it stays in the region of phase space which is inside the separatrix defined by the condition

$$\frac{p^2}{2m} = V_0 \cos(2kz) \tag{3}$$

and illustrated in the figure by the dashed line.

We assume that initially the electrons are uniformly distributed in the z-direction all with the same momentum. Electrons with positive initial momentum on average lose momentum during the interaction, while electrons initially in the lower half of phase space on average gain momentum by absorbing radiation [28, 29]. In order to achieve positive gain the electrons have to be injected with a slightly positive momentum. Moreover, the interaction time should be chosen not too long, in order to ensure that the electrons are not accelerated again and saturation occurs [29]. Figure 1 depicts a situation with a vanishing initial momentum of the electrons. In this case there is no net gain.

2.2. Conditions to enter the quantum regime

We now use this picture to illustrate the transition to the Quantum FEL. We start from the classical limit where the electron momentum is continuous, since the recoil of a single scattering process is negligible.

As we described earlier, this recoil originates from the process when an electron absorbs a wiggler photon and emitts a laser photon, or from the inverse process, and the photons transfer their momenta to the electron due to conservation of momentum. The momenta of the laser photon $\hbar k_{\mathrm{L}}$ and the wiggler photon $\hbar k_{\mathrm{W}}$ add to the total recoil

$$q \equiv \hbar\left(k_{\mathrm{L}} + k_{\mathrm{W}}\right) = 2\hbar k$$

of a single scattering process. In the second step we have used the fact that the wave-numbers for the laser and the wiggler are the same in the Bambini–Renieri frame. The electron can only jump between the rungs of a discrete momentum ladder separated by q.

If we increase the recoil q as shown on the right-hand side of figure 1, where we have indicated by horizontal lines the discrete momentum ladder, we certainly cannot describe the dynamics by continuous trajectories.

We take the separatrix—with the maximal momentum $\pm\sqrt{2mV_0}$—as the typical momentum scale of the FEL dynamics and compare it to the recoil. In the limit $\sqrt{2mV_0}/q \gg 1$ the discreteness of the momentum states certainly does not play an important role and we can take this as the condition for the classical limit of FEL dynamics. However, if we decrease this ratio, quantum mechanics indeed becomes essential.

In fact, the quantity $\sqrt{2mV_0}/q$ is small if the ratio of the important energies, that is the potential height V_0 and the energy $q^2/(2m)$ associated to the recoil, is small. Hence, we can define the quantum parameter

$$\alpha \equiv \frac{V_0/2}{q^2/2m} = \frac{g\sqrt{n}}{\omega_r}$$

as the crucial quantity for the transition from classical to quantum. In the second step we have used the definition of V_0, equation (2), and defined the recoil frequency $\omega_r \equiv q^2/(2m\hbar)$ to rewrite α as the ratio of two frequencies.

For $\alpha \gg 1$ the classical description is valid. However, we are interested in the case of smaller values of α, especially in the limit where $\alpha \ll 1$. In the next sections we show within a quantum mechanical framework, that the infinite momentum ladder reduces in this limit to an effective two-level system.

Besides this condition, arising from the dynamics of the system, we also have to take into account the initial distribution of the electron in momentum space. Due to the Heisenberg uncertainty principle the width Δp of the momentum distribution will always be finite, unless we consider momentum eigenstates. Hence, the rungs of the momentum ladder will broaden with increasing Δp and eventually the discreteness of the momenta will be washed out, even for $\alpha \ll 1$.

Thus, we have to formulate an additional condition for leaving the classical regime and entering the quantum limit: the momentum width Δp should not exceed the separation q of the momentum levels, i.e.

$$\Delta p < q.$$

Indeed, we will show in the next sections, that this requirement is essential to obtain gain in the Quantum FEL.

Having motivated two important requirements for operating an FEL in a quantum regime in an illustrative way, we now develop a quantum description of the FEL dynamics in order to find a rigorous proof of these conditions.

3. Quantum description of the FEL

Every description of the FEL relies on a model of the interaction of relativistic electrons with a co-propagating laser field and a counter-propagating wiggler field. For this purpose we use the framework of a one-dimensional, single-particle theory as proposed in [16]. When we consider the co-moving Bambini–Renieri frame [26] where the frequencies $\omega \equiv ck$ of both the laser and the wiggler field coincide and the motion of the electron can be regarded as nonrelativistic, we find the Hamiltonian

$$\hat{H}' = \frac{\hat{p}^2}{2m} + \hbar g\left(\hat{a}_L^\dagger e^{-i2k\hat{z}} + \hat{a}_L e^{i2k\hat{z}}\right). \tag{4}$$

For a detailed derivation of this Hamiltonian in the Bambini–Renieri frame we refer to appendix B.

As discussed in this appendix, we consider the laser field to be a single quantized mode of the electromagnetic field with the bosonic creation and annihilation operators $\hat{a}_L^\dagger$ and $\hat{a}_L$, respectively, which fulfill the familiar commutation relation $[\hat{a}_L, \hat{a}_L^\dagger] = 1$. The coupling constant

$$g \equiv \frac{1}{\hbar}\frac{e^2}{m}\mathcal{A}_L\tilde{\mathcal{A}}_W,$$

which is derived in appendix B, includes the strength of the wiggler $\tilde{\mathcal{A}}_W$ and the vacuum amplitude $\mathcal{A}_L$ of the laser field, as well as the modified electron mass m, the elementary charge e and the reduced Planck constant $\hbar$. An equivalent Hamiltonian can be derived [17] in the laboratory frame using relativistic quantum electrodynamics.

In the Hamiltonian we have included the mechanical action of both the laser and wiggler fields on the electron by quantizing its motion resulting in the commutation relation $[\hat{z}, \hat{p}] = i\hbar$ for the position $\hat{z}$ and the momentum $\hat{p}$ of the electron. For this reason the annihilation of a laser photon is associated with a momentum displacement operator $\exp(i2k\hat{z})$ leading during the scattering process to a gain of momentum by the amount of the recoil

$$q \equiv 2\hbar k.$$

In complete analogy, the creation of a laser photon leads to a loss of momentum by the amount of $-q$. These recoil effects can be easily understood in terms of Compton scattering as discussed in the introduction.

When we change into the interaction picture, we arrive at the Hamiltonian

$$\hat{H} = \hbar g\left(\hat{a}_L^\dagger e^{-i2k\hat{z}} e^{-i\left(\hat{p}\frac{2k}{m}-\omega_r\right)t} + \hat{a}_L e^{i2k\hat{z}} e^{i\left(\hat{p}\frac{2k}{m}+\omega_r\right)t}\right), \tag{5}$$

where

$$\omega_r \equiv \frac{1}{\hbar}\frac{q^2}{2m} \tag{6}$$

denotes the recoil frequency which is given by the energy associated with the recoil divided by $\hbar$.

The first term of the Hamiltonian from equation (5) suggests that the probability for the emission process is maximized when the momentum $\hat{p}$ of the electron is close to the eigenvalue $p = q/2$ since then the time-dependent phase vanishes. In the spirit of the rotating wave approximation [23] we suspect that this process is suppressed when the oscillation is too rapid. This suspicion is in accordance with the results presented in the next sections.

To emphasize these resonances we introduce the momentum-dependent detunings

$$\Delta_j = \Delta_j(p) \equiv 2\omega_r\left(\frac{p}{q} - \frac{1}{2} - j\right), \tag{7}$$

and the Hamiltonian from equation (5) takes the form

$$\hat{H} = \hbar g\left(\hat{a}_L^\dagger e^{-i2k\hat{z}} e^{-i\Delta_0(\hat{p})t} + \hat{a}_L e^{i2k\hat{z}} e^{i\Delta_{-1}(\hat{p})t}\right). \tag{8}$$

In the following sections we discuss two different ways to perturbatively solve the Schrödinger equation with this Hamiltonian.

4. Emergence of the Quantum FEL: standard perturbation theory

Our first approach to solve for the dynamics dictated by the Hamiltonian, equation (8), uses the expansion of the time-evolution operator $\hat{\mathcal{U}}(t)$ that evolves an initial state $|\psi(0)\rangle$ for a time t via the relation

$$|\psi(t)\rangle = \hat{\mathcal{U}}(t)|\psi(0)\rangle. \tag{9}$$

For short times, that is for $g\sqrt{n+1}\ t \ll 1$ with the photon number n, we arrive at the expansion

$$\hat{\mathcal{U}}(t) = \mathbb{1} + \hat{\mathcal{U}}_1(t) + \hat{\mathcal{U}}_2(t) + \cdots \tag{10}$$

with the first-order contribution

$$\hat{\mathcal{U}}_1(t) \equiv -\frac{i}{\hbar}\int_0^t dt_1 \hat{H}\left(t_1\right),$$

and the contribution in second-order

$$\hat{\mathcal{U}}_2(t) \equiv -\frac{i}{\hbar}\int_0^t dt_2 \hat{H}\left(t_2\right)\hat{\mathcal{U}}_1\left(t_2\right), \tag{11}$$

as for example shown in [23] in an iterative procedure. We first discuss the first-order processes and their implications for the quantum regime, before we then turn to the second-order processes.

4.1. First-order processes

We expand a generic state

$$|\psi(t)\rangle \equiv \int_{-\infty}^{\infty} dp \sum_{n=0}^{\infty} c_n(p,\, t)|n,\, p\rangle \tag{12}$$

into photon number states $|n\rangle$ of the laser field and momentum eigenstates $|p\rangle$ of the electron with the corresponding expansion coefficients $c_n(p,\, t)$.

We use this representation in the time evolution from equation (9) to equate the probability amplitudes $c_n(p,\, t)$. In this way, we arrive with $|\psi(t)\rangle \cong (\mathbb{1} + \hat{\mathcal{U}}_1)|\psi(0)\rangle$ at the time evolution

$$c_\mu(p;\, t) = c_\mu(p;\, 0) - ig\int_0^t dt_1\left[\sqrt{n+\mu+1}\, e^{i\Delta_\mu t_1} c_{\mu+1}(p;\, 0) + \sqrt{n+\mu}\, e^{-i\Delta_{\mu-1}t_1} c_{\mu-1}(p;\, 0)\right].$$

Here, we have recalled the definition of the detuning Δ_j from equation (7) and have introduced the abbreviation

$$c_\mu(p;\, t) \equiv c_{n+\mu}(p - \mu q,\, t). \tag{13}$$

This convenient notation reflects the fact that in the Hamiltonian $\hat{H}$ defined in equation (8), the creation of a laser photon is always associated with a loss of momentum by the amount of q, whereas the annihilation of a laser photon always goes along with a gain in momentum by q. Hence, μ corresponds to the number of created photons, which is again associated with a recoil of $-\mu q$. In this sense the coefficients $c_\mu(p;\, t)$ as defined in equation (13) can be interpreted in terms of the so-called *scattering basis* [15].

We now perform the integration over time and find the relation

$$c_\mu(p;\, t) = c_\mu(p;\, 0) - igt\sqrt{n+\mu+1}\, e^{i\Delta_\mu t/2}\mathrm{sinc}\left(\frac{\Delta_\mu t}{2}\right) c_{\mu+1}(p;\, 0) \tag{14}$$

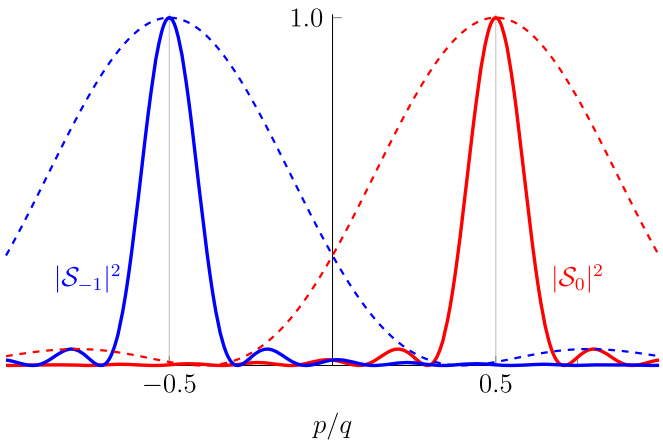

Figure 2. Momentum-selectivity functions $|\mathcal{S}_0|^2$ (red) and $|\mathcal{S}_{-1}|^2$ (blue) for the probability densities $|c_1|^2$ and $|c_{-1}|^2$ of gaining and losing a photon according to equation (18). The dashed lines are for $\omega_r t = 3.5$, the solid ones for $\omega_r t = 15$. We recognize distinct resonances at the values $p = q/2$ for gain and $p = -q/2$ for loss, which become sharper for increasing values of $\omega_r t$. For sufficiently large $\omega_r t$ a gain and a loss interval in momentum emerges since the functions $|\mathcal{S}_0|^2$ and $|\mathcal{S}_{-1}|^2$ become well separated. This separation is a necessary condition for the quantum regime of the FEL.

$$- \mathrm{i}gt\sqrt{n+\mu}\,\mathrm{e}^{-\mathrm{i}\Delta_{\mu-1}t/2}\mathrm{sinc}\left(\frac{\Delta_{\mu-1}t}{2}\right)c_{\mu-1}(p;\,0)$$

in which the corrections to the probability amplitude $c_\mu(p;\,0)$ scale linearly in the expansion parameter $g\sqrt{n+1}t$.

To obtain the emission and absorption probabilities we now choose the Fock state $|n\rangle$ as the initial condition for the laser field, and the initial wave function $\phi(p)$ of the electron in momentum representation. With the initial values

$$c_\mu(p;\,0) = \delta_{0,\mu}\phi(p) \tag{15}$$

we find from equation (14) the probability density

$$\left|c_{+1}(p;\,t)\right|^2 = g^2(n+1)t^2\left|\mathcal{S}_0\right|^2|\phi(p)|^2 \tag{16}$$

of gaining a photon, as well as the probability density

$$\left|c_{-1}(p;\,t)\right|^2 = g^2nt^2\left|\mathcal{S}_{-1}\right|^2|\phi(p)|^2 \tag{17}$$

of losing a photon. Here, we have introduced the momentum-selectivity functions

$$\left|\mathcal{S}_\mu\right|^2 \equiv \mathrm{sinc}^2\left(\frac{\Delta_\mu t}{2}\right). \tag{18}$$

In order to find the probabilities for the single-photon transition the functions $|\mathcal{S}_\mu|^2 = |\mathcal{S}_\mu(p)|^2$ are weighted with the initial momentum distribution $|\phi(p)|^2$ and we have to integrate over p.

The selectivity functions are displayed in figure 2 for $\mu = 0,\ 1$ and show that resonances occur at $p = q/2$ for gain, and $p = -q/2$ for loss. Moreover, for increasing values of $\omega_r t$ the width of these resonances decreases, leading for sufficiently large values, that is for $1 \ll \omega_r t$ to well-separated intervals.

4.2. Second-order processes

However, so far we have not addressed the role of higher-order processes. For this reason we turn to the next higher-order expansion of equation (10) and find a condition for the suppression of two-photon processes beyond the condition $1 \ll \omega_r t$.

The integrations necessary to calculate the matrix element $\langle n+\mu,\ p-\mu q|\ \hat{\mathcal{U}}_2(t)|\psi(0)\rangle$ using equation (11) are performed in appendix C and lead to contributions to the time-evolved coefficient $c_\mu(p;\,t)$ from equation (14) that stem from two-photon processes.

We again choose equation (15) as the initial condition for our problem and according to appendix C we find

$$\left|c_{+2}(p;\,t)\right|^2 = g^2(n+2)t^2\left(\frac{g\sqrt{n+1}}{\omega_r}\right)^2\left|\mathcal{E}_{+2}\right|^2|\phi(p)|^2 \tag{19}$$

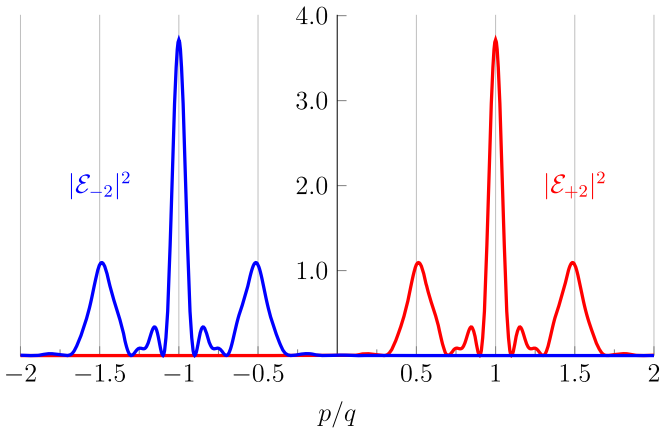

Figure 3. Momentum selectivity functions $|\mathcal{E}_{+2}|^2$ (red) and $|\mathcal{E}_{-2}|^2$ (blue) given by equations (20) and (22), respectively and determining the probability densities $|c_{+2}|^2$ and $|c_{-2}|^2$ defined by equations (19) and (21) of gaining two photons and losing two photons for $\omega_r t = 15$. We see distinct dominant resonances at the values $p = q$ for gain and $p = -q$ for loss. Additional resonances appear at $p = \pm q/2$, which represent the resonances of the one-photon transition, and at $p = \pm 3q/2$.

for the probability density of a two-photon gain with the momentum-selectivity function

$$\left|\mathcal{E}_{+2}\right|^2 \equiv \frac{1}{\left(\frac{p}{q}-\frac{1}{2}\right)^2}\left[\operatorname{sinc}^2\left(\Delta_{\frac{1}{2}}t\right)+\operatorname{sinc}^2\left(\frac{\Delta_1 t}{2}\right)-2\operatorname{sinc}\left(\Delta_{\frac{1}{2}}t\right)\operatorname{sinc}\left(\frac{\Delta_1 t}{2}\right)\cos\left(\frac{\Delta_0 t}{2}\right)\right]. \tag{20}$$

Likewise, we obtain in appendix C the probability density

$$\left|c_{-2}(p;t)\right|^2 = g^2(n-1)t^2\left(\frac{g\sqrt{n}}{\omega_r}\right)^2\left|\mathcal{E}_{-2}\right|^2|\phi(p)|^2 \tag{21}$$

of losing two photons with the corresponding selectivity function

$$\left|\mathcal{E}_{-2}\right|^2 \equiv \frac{1}{\left(\frac{p}{q}+\frac{1}{2}\right)^2}\left[\operatorname{sinc}^2\left(\Delta_{-\frac{3}{2}}t\right)+\operatorname{sinc}^2\left(\frac{\Delta_{-2}t}{2}\right)-2\operatorname{sinc}\left(\Delta_{-\frac{3}{2}}t\right)\operatorname{sinc}\left(\frac{\Delta_{-2}t}{2}\right)\cos\left(\frac{\Delta_{-1}t}{2}\right)\right]. \tag{22}$$

The functions $|\mathcal{E}_{+2}|^2$ and $|\mathcal{E}_{-2}|^2$ displayed in figure 3 for $\omega_r t = 15$ show dominant resonances at $p = q$ and $p = -q$. Additional resonances appear at $p = \pm q/2$—the resonances of the single-photon transition as depicted in figure 2—and at $p = \pm 3q/2$. Hence, even for sufficiently large $\omega_r t \gg 1$, where both $|\mathcal{S}_0|^2$ and $|\mathcal{S}_{-1}|^2$ are well separated and the initial momentum distribution is concentrated around a single-photon resonance, i.e. $p = \pm q/2$, there might be a non-negligible probability for a two-photon process to occur. Hence, this system does not necessarily behave like a two-level system.

4.3. The emergence of the quantum parameter

However, we note in equations (19) and (21) the factor $(g\sqrt{n+1}/\omega_r)^2 \cong (g\sqrt{n}/\omega_r)^2$. Therefore, we define the *quantum parameter*

$$\alpha \equiv \frac{g\sqrt{n+1}}{\omega_r}, \tag{23}$$

which is the ratio of the two relevant frequency scales, that is the coupling strength $g\sqrt{n+1}$ and the recoil frequency ω_r defined in equation (6).

As discussed in the preceding section, for $1 \ll \omega_r t$ we have a clear separation into a loss and gain interval. Additionally, the expansion is just valid in the short-time limit, more precisely for $g\sqrt{n+1}\,t \ll 1$ giving rise to a regime where the quantum parameter α is a small quantity, that is

$$\alpha \ll 1. \tag{24}$$

This condition defines the quantum regime of the FEL.

In this case two-photon transitions can be neglected in comparison to the single-photon process around the resonances $p = \pm q/2$. With a similar reasoning higher multi-photon transitions are not of importance—in contrast to the classical regime [1] of the FEL. Most importantly we have two separated intervals of gain and loss and are thus able to treat the Quantum FEL as a two-level system in momentum space.

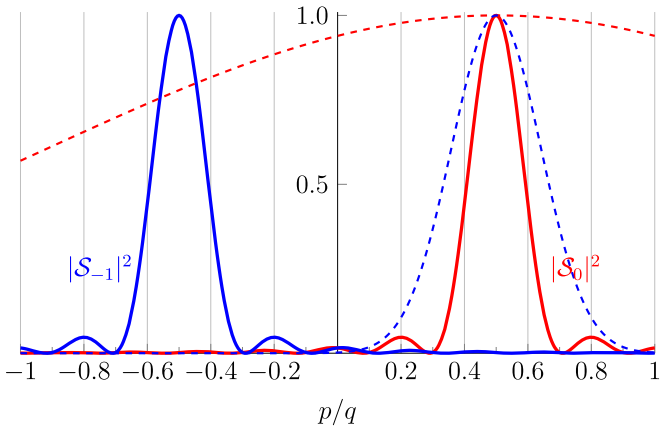

Figure 4. Different initial momentum distributions for the Quantum FEL. The selectivity functions $|\mathcal{S}_0|^2$ of gaining and $|\mathcal{S}_{-1}|^2$ of losing a photon are plotted for scale. The blue dashed distribution is a Gaussian with a momentum width ($\Delta p = q/5$) that lies within the borders of $|\mathcal{S}_0|^2$ and has practically no overlap with $|\mathcal{S}_{-1}|^2$. Therefore, the probability of gaining photons exceeds the probability of losing photons. In contrast, the dashed red distribution is a Gaussian with a width ($\Delta p = 5q$) that has a significant overlap with $|\mathcal{S}_0|^2$ as well as with $|\mathcal{S}_{-1}|^2$, leading to a reduced gain.

4.4. Gain of Quantum FEL requires narrow momentum distribution

Having obtained an effective two-level system in the quantum regime with the excited state $|q/2\rangle$ and the ground state $|-q/2\rangle$, we can connect the Quantum FEL to the one-atom maser [23, 24] and employ familiar concepts of standard laser theory.

However, a conventional laser needs a population inversion [30]. In the case of the Quantum FEL we now find a condition to achieve this population inversion. Indeed, this requirement is associated with the initial momentum distribution.

Since the probability densities $|c_{+1}|^2$ and $|c_{-1}|^2$ of gaining and losing a photon, given by equations (16) and (17), are governed by the selectivity functions $|\mathcal{S}_\mu|^2$, defined by equation (18), the momentum spread of the electrons is of utmost importance. To achieve inversion the excited state defined by the selectivity function $|\mathcal{S}_0|^2$ needs to have a higher population than the ground state defined by $|\mathcal{S}_{-1}|^2$. Since their maxima are separated by q the momentum distribution has to vary significally on the scale of the recoil.

If we assume a Gaussian distribution in the momentum with a width Δp, we require the relation

$$\left(\frac{\Delta p}{q}\right) < 1 \tag{25}$$

in order to achieve positive gain.

The reason for this condition can be seen from figure 4 where we show two Gaussian momentum distributions with different widths Δp. A small width results in the majority of electrons emitting radiation according to the selectivity function $|\mathcal{S}_0|^2$. In contrast, a broad momentum distribution covers both, $|\mathcal{S}_{-1}|^2$ and $|\mathcal{S}_0|^2$, resulting in equal probabilities for emission and absorption and therefore no population inversion and no gain. An analogous requirement for the momentum spread of the electrons was derived in [31].

5. Emergence of the Quantum FEL: method of averaging

In contrast to the expansion used in the previous section to develop an analytic theory of the Quantum FEL, valid in the short-time limit, we employ in this section a different approach which also is true for larger times. First, we note that the model of a non-relativistic particle interacting with quantized light fields as described by the Hamiltonian, equation (8), is very similar to atomic Bragg diffraction, where matter waves are scattered from a periodic potential, usually appropriately formed by a classical standing light wave. This phenomenom has been experimentally observed in [32].

In contrast, the well-known crystallographic Bragg diffraction of X-rays is the process where light waves are scattered from a crystal lattice. In this case, the light waves are diffracted into certain angles, if a resonance condition—the so called Bragg condition—is fulfilled [33]. In atomic Bragg diffraction this condition causes a diffraction into preferred momenta, i.e. the atom experiences a momentum kick if the initial momentum is close to the resonance condition. In general, only two momentum states are relevant.

In this section, we discuss the regime in which such a reduction of the momentum states is possible. In particular, we use the method of averaging introduced in [22] and in detail explained and employed to atomic

Bragg diffraction in [34], to adiabatically remove all but two momentum states. In appendix D we briefly recapitulate this method and apply it to the FEL.

We now use the results of the method of averaging to show that the quantum regime of the FEL emerges when the ratio of the two relevant frequencies, that is the interaction strength g of the scattering process and the recoil frequency ω_r, is sufficiently small. This condition is in complete agreement with the discussion of the previous section. In this case, the suppression of different momentum states can be easily understood as a consequence of energy–momentum conservation.

5.1. Three-term recurrence relation

To apply the method of averaging, we first have to find a differential equation for the expansion coefficients c_μ of an arbitrary state and bring it into the form of the Bragg diffraction situations analyzed in [34]. For this purpose, we use the Schrödinger equation

$$\mathrm{i}\hbar\frac{\mathrm{d}}{\mathrm{d}t}\,|\psi(t)\rangle = \hat{H}\,|\psi(t)\rangle$$

with the Hamiltonian $\hat{H}$ defined in equation (8) and the generic state $|\psi(t)\rangle$ in the representation of equation (12) and we arrive at the three-term recurrence relation

$$\mathrm{i}\dot{c}_\mu = g\Big[\sqrt{n+\mu+1}\,\mathrm{e}^{\mathrm{i}\Delta_0 t}\mathrm{e}^{-\mathrm{i}2\mu\omega_r t}c_{\mu+1} + \sqrt{n+\mu}\,\mathrm{e}^{-\mathrm{i}\Delta_0 t}\mathrm{e}^{\mathrm{i}2(\mu-1)\omega_r t}c_{\mu-1}\Big], \tag{26}$$

for the coefficients $c_\mu \equiv c_{n+\mu}(p-\mu q,\,t)$. Here, we have used the relations

$$\Delta_\mu = \Delta_0 - 2\mu\omega_r \text{ and } \Delta_{\mu-1} = \Delta_0 - 2(\mu-1)\omega_r$$

following directly from the definition of the detuning Δ_j in equation (7).

The differential equation, equation (26), describes the exact time evolution according to the FEL Hamiltonian, equation (8). The method of averaging we are about to apply plays with different time scales of the dynamics and separates them into slow large-amplitude resonant oscillations, and rapidly oscillating small-amplitude corrections. Since the phase factors in equation (26) are momentum dependent, the approximate solutions found by this method depend on the initial momenta.

5.2. Two-level approximation: Rabi oscillations

We are interested in a behavior reminiscent of a two-level system. Thus we concentrate on momenta that are close to half-integer multiples of q. They yield in lowest approximation single-photon transitions when we apply the method of averaging as in [34].

When we interpret the coefficients c_μ in equation (26) as components of a vector $\boldsymbol{c}$, we can cast equation (26) into the form

$$\mathrm{i}\dot{\boldsymbol{c}} = \varepsilon\left(\mathcal{H}_0 + \sum_{\nu\neq 0}\mathrm{e}^{\mathrm{i}\nu\omega_r t}\mathcal{H}_\nu\right)\boldsymbol{c}\,, \tag{27}$$

where we have introduced the expansion parameter $\varepsilon \equiv g/\omega_r$ and the matrix elements of the Hamiltonian are defined by

$$\left(\mathcal{H}_\nu\right)_{\mu,\mu'} \equiv \sqrt{n+\mu+1}\;\omega_r\mathrm{e}^{\mathrm{i}\Delta_0 t}\delta_{2\mu,-\nu}\;\delta_{\mu+1,\mu'} + \sqrt{n+\mu}\;\omega_r\mathrm{e}^{-\mathrm{i}\Delta_0 t}\delta_{2(\mu-1),\nu}\;\delta_{\mu-1,\mu'}. \tag{28}$$

In this representation, the structure of the oscillatory terms stands out most clearly. The Hamiltonian matrices $\mathcal{H}_\nu$ are multiplied by phase factors oscillating with multiples of the recoil frequency ω_r. These rapidly varying terms are suppressed if $g\sqrt{n+1} \ll \omega_r$, and may be, e.g. as it is usually done in the rotating wave approximation (see for example in [23]), neglected.

First, we choose $p = q/2$, i.e. $c_\mu(p;\,t=0) = \delta_{\mu,0}\,\delta(p-q/2)$, to find the resonant solution. The reason for this resonance can be seen in figure 5. In this case, the kinetic energy $(q/2)^2/(2m)$ of the particle is equal to the energy of the scattered particle with momentum $p-q=-q/2$. Moreover, this is the only resonant single-photon process that fulfills both energy and momentum conservation.

Since $\Delta_0(q/2) = 0$, the matrices $\mathcal{H}_\nu$ defined by equation (28) become time independent, and we find

$$\mathcal{H}_0 = \sqrt{n+1}\;\omega_r\begin{pmatrix}0&0&0&0\\0&0&1&0\\0&1&0&0\\0&0&0&0\end{pmatrix},$$

where we have just focused on the four momentum states $(-3q/2,\,-q/2,\,+q/2,\,+3q/2)$ giving rise to the vector $\boldsymbol{c} = (c_{-1},\,c_0,\,c_1,\,c_2)^{\mathrm{T}}$ of probability amplitudes corresponding to $(c_{n-1}(3q/2),\,c_n(q/2),\,c_{n+1}(-q/2),\,c_{n+2}(-3q/2))$in the basis of equation (12).

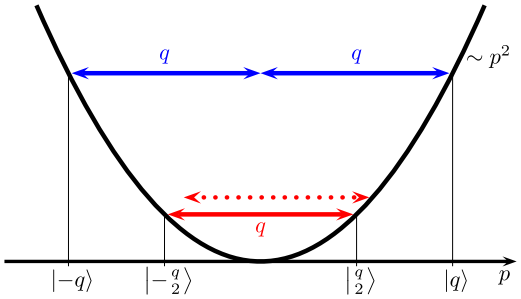

Figure 5. Resonances in the Quantum FEL. During the scattering process the electrons experience a recoil q and perform Rabi oscillations between two momentum states. Due to energy conservation, both states are on the kinetic energy parabola (red solid line) and thus resonantly connected. Deviations from this resonance lead to a detuned Rabi oscillation (red dotted line). A resonant second-order process (blue lines) needs a non-resonant level and hence is suppressed.

With this special form of $\mathcal{H}_0$ and time-independent $\mathcal{H}_\nu$, the solution of equation (27) reads according to [34] up to zeroth order in ε

$$\boldsymbol{c}(t) = \exp\left(-\mathrm{i}\varepsilon\mathcal{H}_0 t\right)\boldsymbol{c}(0) = \begin{pmatrix} 1 & 0 & 0 & 0 \\ 0 & \cos\left(g\sqrt{n+1}\ t\right) & -\mathrm{i}\sin\left(g\sqrt{n+1}\ t\right) & 0 \\ 0 & -\mathrm{i}\sin\left(g\sqrt{n+1}\ t\right) & \cos\left(g\sqrt{n+1}\ t\right) & 0 \\ 0 & 0 & 0 & 1 \end{pmatrix}\boldsymbol{c}(0). \tag{29}$$

Hence, Rabi oscillations occur between the two momenta $q/2$ and $-q/2$, whereas the populations of the higher momenta $\pm 3q/2$ remain unchanged. This process corresponds to the red solid arrow in figure 5.

We emphasize that according to [34], the solution, equation (29), fulfills an approximate differential equation which corresponds to equation (27) up to zeroth order in the parameter $\alpha \equiv \varepsilon\sqrt{n+1} = g\sqrt{n+1}/\omega_\mathrm{r}$. Hence, it is a valid approximation only for $\alpha \ll 1$. In cold atom physics, this regime is called the *deep Bragg regime* [34]. In the context of our discussion we refer to it as the *quantum regime* of the FEL, which is why we call α the quantum parameter.

The solution obtained so far is the slowly oscillating, resonant solution. In lowest-order approximation, we can include small-amplitude rapidly oscillating off-resonant corrections. They correspond to off-resonant single-photon processes and lead to populations in the momentum states $\pm 3q/2$. We will discuss these corrections, whose amplitude scales with α, in the next section.

Multi-photon processes like the two-photon transition shown in figure 5 from q to $-q$ (blue lines) can be calculated by setting the initial momentum to $p = q$ and go to the next higher order of the method of averaging. However, even for the situation of our interest, where $p = q/2$, we find resonant multi-photon situations for the transition $q/2$ to $-q/2$ like e.g. the three-photon processes using $3q/2$ or $-3q/2$ as a virtual level. The resulting corrections can be calculated in third order of the method of averaging. We will discuss them in greater detail in the next section.

However, we want to emphasize that they occur on a time scale which is much longer than the one-photon process in the quantum regime since its frequency scales with $\alpha^2 g\sqrt{n+2}$ in contrast to $g\sqrt{n+1}$.

So far, we have just considered the exact resonance at $p = q/2$ with the detuning $\Delta_0 = 0$. We now turn to deviations from this resonance. Hence, for $p \neq q/2$ the time-dependent phase factors are not unity. According to [34], a good approximation can be found if the time dependence of $\mathcal{H}_\nu$ can be neglected in comparison to ω_r, i.e. we find

$$\frac{|\Delta_0|}{\omega_\mathrm{r}} = 2\left|\frac{p}{q} - \frac{1}{2}\right| \ll 1,$$

which means that p has to be in the vicinity of $q/2$.

To find a more convenient description of the Hamiltonian matrices $\mathcal{H}_\nu$ in the neighborhood of the resonance $q/2$, we use the transformation

$$\begin{pmatrix} \tilde{c}_0 \\ \tilde{c}_1 \end{pmatrix} \equiv \begin{pmatrix} \mathrm{e}^{-\mathrm{i}\Delta_0 t/2} c_0 \\ \mathrm{e}^{\mathrm{i}\Delta_0 t/2} c_1 \end{pmatrix} \tag{30}$$

and arrive at

$$\tilde{\mathcal{H}}_0 = \begin{pmatrix} \Delta_0/2 & g\sqrt{n+1} \\ g\sqrt{n+1} & -\Delta_0/2 \end{pmatrix},$$

with the solution [34]

$$\tilde{\boldsymbol{c}}(t) = \exp\left(-\mathrm{i}\tilde{\mathcal{H}}_0 t\right)\tilde{\boldsymbol{c}}(0) = \left[\cos\Omega_n t\,\mathbb{1} - \mathrm{i}\frac{\sin\Omega_n t}{\Omega_n}\begin{pmatrix} \Delta_0/2 & g\sqrt{n+1} \\ g\sqrt{n+1} & -\Delta_0/2 \end{pmatrix}\right]\tilde{\boldsymbol{c}}(0), \tag{31}$$

where $\mathbb{1} \equiv \delta_{\mu,\mu'}$ denotes the identity operator and

$$\Omega_n \equiv \sqrt{g^2(n+1) + \left(\frac{\Delta_0}{2}\right)^2} \tag{32}$$

is the Rabi frequency.

Hence, a deviation from $p = q/2$ yields a detuning of the Rabi oscillation, which can be understood already from figure 5. Indeed, the dotted red line shows that for a deviation from the momentum $q/2$ there is no resonant transition, and for this momentum there will be a faster, but suppressed oscillation as suggested by energy-time uncertainty, giving rise to the detuning term in equations (31) and (32).

In cold atom physics, this effect is called [35] *velocity selectivity*, since just particles around the resonant momenta are scattered and the oscillations of other momentum states are suppressed. Of course the analytical solution presented here is just valid for small deviations from resonance, but the suppression of the oscillations can easily be understood. A numerical solution of equation (27) also shows this velocity selectivity but yields a more accurate description of the width of the resonance [34, 36].

We now sketch how the condition equation (25) on the width Δp of the momentum distribution can be understood within the framework of the method of averaging. Due to the velocity selectivity only momenta close to resonances, i.e. integer multiples of $q/2$, will participate in the interaction. If we turn to the case $p \sim -q/2$ we find the same two-level system as for $p \sim +q/2$. However, now the electron is initially in the ground state and will absorb photons to get into the excited state.

Hence, if the momentum distribution covers both resonances, the velocity selectivity picks out the emission process *and* the absorption process and we obtain zero gain, just like in the case of ordinary perturbation theory discussed in section 4.4. Thus, we require a narrow initial momentum distribution, i.e. $\Delta p < q$, centered around the resonance $p = +q/2$ to realize the quantum FEL.

5.3. Higher-order terms: shifts and amplitude corrections

We now calculate higher-order corrections to the two-level approximation of the Quantum FEL in the framework of the method of averaging. In this way, we can show how the two-level behavior emerges as we decrease the quantum parameter α. This example demonstrates the power of the method of averaging for problems with two different time scales.

In order to simplify our approach we restrict ourselves to the resonant case $p = q/2$, i.e. we use the initial condition equation (15) and assume that the initial wave function $\phi(p)$ of the electron is the momentum eigenfunction with the eigenvalue $q/2$ resulting in

$$c_\mu(t=0) = \delta_{\mu,0}\delta(p - q/2).$$

According to the previous section the probability amplitudes of zeroth order in α are given by equation (29) and we only have to take the modulus square to arrive at the probability to find the electron in a given momentum state. For the excited state that is $\mu = 0$ this probability reads

$$\left|c_0(t)\right|^2 = \cos^2\left(\Omega_n t\right), \tag{33}$$

where we have used our initial condition and have written the solution in terms of the Rabi frequency $\Omega_n = g\sqrt{n+1}$ for zero detuning. As stated in the previous section, equation (33) describes the Rabi oscillations of a two-level system.

To obtain the corrections to this zeroth-order solution, we have to modify ordinary perturbation theory in a way explained in detail in [34] and shown for the problem of the Quantum FEL in appendix D. According to equation (D.8) we find the modification

$$\left|c_0(t)\right|^2 = \cos^2\left[\left(\Omega_n - \chi\right)t\right] - \frac{\alpha^2}{2}\cos\left[\left(\Omega_n - \chi\right)t\right] \times \left(\cos\left[\left(\Omega_n - \chi\right)t\right] - \cos\left(\chi t\right)\cos\left[2\omega_r t\left(1 + \frac{3\alpha^2}{8}\right)\right]\right), \tag{34}$$

of equation (33), where we have included contributions in the next higher order for the amplitude and the shift

$$\chi \equiv \frac{\alpha^2}{4}\Omega_n$$

of the Rabi frequency which scale both with α^2.

To emphasize the accuracy of our method we now compare our results to a numerical solution of the dynamical equations for the coefficients c_μ. Therefore, we return to the Hamiltonian, equation (4), in the Schrödinger picture, which for $p = q/2$ yields immediately the differential equation

$$\mathrm{i}\dot{c}_\mu(t) = \omega_r\left(\mu - \frac{1}{2}\right)^2 c_\mu(t) + g\sqrt{n+\mu+1}\; c_{\mu+1}(t) + g\sqrt{n+\mu}\; c_{\mu-1}(t). \tag{35}$$

This set of equations can be solved by diagonalizing a matrix with nonzero elements on the diagonal as well as on the sub- and super-diagonal as apparent from equation (35). For our simulations we have used $n = 1000$ and have truncated the recurrence relation at $\mu = -49$ and $\mu = 50$.

In the upper part of figure 6 we compare our analytical expressions for $|c_0(t)|^2$, equations (33) and (34), obtained by the method of averaging to the numerical results for a relatively high value of the quantum parameter, that is for $\alpha = 0.5$. This choice of α was made to test the validity of our approximation even beyond the deep quantum regime.

Although for short times the lowest order solution, equation (33), agrees well with the numerical curve, for larger times it starts to deviate. This deviation results from a frequency shift in the Rabi oscillation and a modulation in the amplitude. However, already in the next higher approximation, equation (34), which contains these modifications there is very good agreement between the analytical and the numerical result.

5.4. Approach towards two-level system

When we decrease the value of α further to 0.1 as shown in the lower part of figure 6, we expect to see Rabi oscillations corresponding to a two-level system. Indeed, we discover that already the lowest approximation, equation (33), which corresponds to the two-level approximation is in very good agreement with the numerical solution. We take this behavior as evidence that the two-level behavior of the Quantum FEL becomes more and more prominent for decreasing values of α.

However, not only the excited and the ground state, $\mu = 0$ and $\mu = 1$, are of interest, when we want to study the transition from the infinite momentum ladder to a two-level system, but we have to also verify that transitions to other levels, e.g. to the next neighboring states defined by $\mu = -1$ and $\mu = 2$ are suppressed. In the zeroth order of the method of averaging we cannot make any statement about these transitions. However, in the next higher order these neighboring levels appear, as shown in appendix D.

In figure 7 we compare the analytical expression

$$\left|c_{-1}(t)\right|^2 = \frac{\alpha^2}{4}\left(\cos^2\left(\chi t\right) + \cos^2\left[\left(\Omega_n - \chi\right)t\right] - 2\cos\left(\chi t\right)\cos\left[\left(\Omega_n - \chi\right)t\right]\cos\left[\left(1 + \frac{3\alpha^2}{8}\right)2\omega_r t\right]\right), \tag{36}$$

derived in appendix D with the numerically obtained solution of equation (35) for $\alpha = 0.1$. Both curves agree very well and basically consist of rapid oscillations, which are modulated by a beat frequency which matches roughly the Rabi frequency Ω_n of the two-level system. Moreover, according to equation (36) the amplitude of these oscillations scales with α^2. The same statement is correct for the probability $|c_2(t)|^2$ to be in the state $\mu = 2$, equation (D.9), which is shown in appemdix D. Hence, for small values of α we can neglect the contributions from the levels $\mu = -1$ and $\mu = 2$.

Since we develop in our method an asymptotic expansion in the quantum parameter α, other levels, which appear in higher orders of our approach, scale with even higher powers of α. Thus, their population is even more suppressed in comparison to the one of the direct neighbors of the states $\mu = 0$ and $\mu = 1$. Hence, for $\alpha \ll 1$ we can really identify the FEL dynamics as the one in which the momentum ladder reduces to a two-level system.

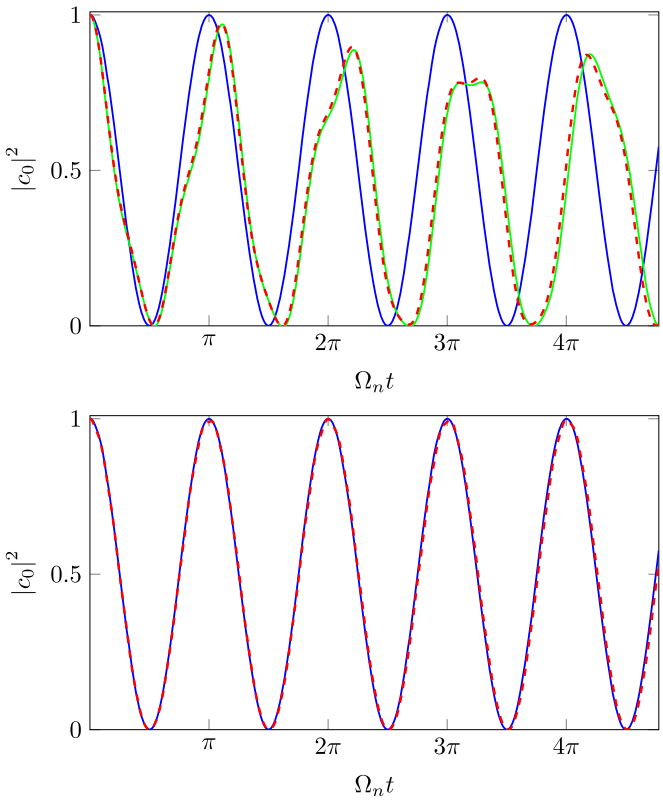

Figure 6. Probability $|c_0|^2$ to be in the 'excited' state $\mu = 0$ as a function of the scaled time $\Omega_n t$ according to the two-level approximation, equation (33), (green line) and the next higher order of the method of averaging, equation (34) (blue line) compared to the numerical solution of equation (35) (red dashed line). Although the zeroth order fits for $\alpha = 0.5$ (top) hardly the numerical results, already the first correction provides us with an excellent agreement. In contrast to that, for $\alpha = 0.1$ (bottom) already the lowest approximation agrees very well with the simulation and we omit higher order corrections.

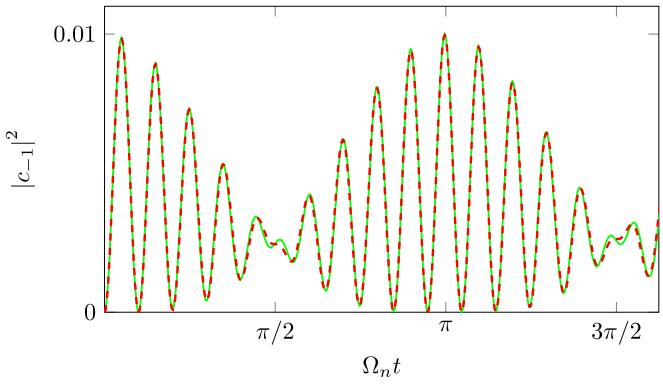

Figure 7. Probability $|c_{-1}|^2$ to be in the level $\mu = -1$ as a function of the scaled time $\Omega_n t$ according to the method of averaging, equation (36), (green line) compared to the numerical solution of equation (35) (red dashed line) for $\alpha = 0.1$. We obtain fast oscillations which are modulated by a beat frequency roughly equal to the Rabi frequency Ω_n of the two-level system.

5.5. Link to short-time limit

We conclude this section by connecting the results obtained by the method of averaging to the ones of section 4. Therefore, we restrict ourselves to the lowest-order of the method of averaging, equation (31), which includes the effects of a small deviation from resonance.

The method of averaging uses an approximate Hamiltonian to solve the Schrödinger equation exactly, whereas in the expansion for short times we have used the exact Hamiltonian but found an approximate solution of the Schrödinger equation. Thus, we expect a better long-time behavior of the results achieved by the method of averaging compared to the ones obtained by ordinary perturbation theory.

A Taylor expansion of the solution, equation (31), obtained by the method of averaging for small $\xi \equiv g\sqrt{n+1}\,t$, i.e.

$$\tilde{\boldsymbol{c}}(t) \cong \tilde{\boldsymbol{c}}(t)|_{\xi=0} + \frac{\partial}{\partial\xi}\tilde{\boldsymbol{c}}(t)\Big|_{\xi=0}\xi + \cdots$$

yields

$$\tilde{\boldsymbol{c}}(t) \cong \begin{pmatrix} \mathrm{e}^{-\mathrm{i}\Delta_0 t/2} & -\mathrm{i}g\sqrt{n+1}\,t\,\mathrm{sinc}\dfrac{\Delta_0 t}{2} \\ -\mathrm{i}g\sqrt{n+1}\,t\,\mathrm{sinc}\dfrac{\Delta_0 t}{2} & \mathrm{e}^{\mathrm{i}\Delta_0 t/2} \end{pmatrix}\tilde{\boldsymbol{c}}(0),$$

which together with the transformation equation (30), leads us to

$$c_0^{(\mathrm{ma})}(p;\,t) \cong c_0(p;\,0) - \mathrm{i}g\sqrt{n+1}\,t\mathrm{e}^{\mathrm{i}\Delta_0 t/2}\mathrm{sinc}\frac{\Delta_0 t}{2}c_1(p;\,0)$$

and

$$c_1^{(\mathrm{ma})}(p;\,t) \cong c_1(p;\,0) - \mathrm{i}g\sqrt{n+1}\,t\mathrm{e}^{-\mathrm{i}\Delta_0 t/2}\mathrm{sinc}\frac{\Delta_0 t}{2}c_0(p;\,0).$$

Here, we have introduced the superscript (ma) to indicate that the form of these coefficents originates from the method of averaging.

To compare these expressions to the corresponding coefficients calculated by the first-order perturbation theory in the short-time limit (superscript (pt)), we recall our results from equation (14) and find

$$c_0^{(\mathrm{pt})}(p;\,t) \cong c_0^{(\mathrm{ma})}(p;\,t) - \mathrm{i}g\sqrt{n}\,t\mathrm{e}^{-\mathrm{i}\Delta_{-1}t/2}\mathrm{sinc}\frac{\Delta_{-1}t}{2}c_{-1}(p;\,0)$$

and

$$c_1^{(\mathrm{pt})}(p;\,t) \cong c_1^{(\mathrm{ma})}(p;\,t) - \mathrm{i}g\sqrt{n+2}\,t\mathrm{e}^{\mathrm{i}\Delta_1 t/2}\mathrm{sinc}\frac{\Delta_1 t}{2}c_2(p;\,0).$$

Hence, in contrast to the Taylor expansion of the solution obtained by the method of averaging, we now have additional couplings to other momentum states. However, for sufficiently large $\omega_{\mathrm{r}}t$, we see that the sinc-functions hardly overlap and one of these transitions will be dominant for a particular momentum.

It is not surprising that this way of perturbatively solving the Schrödinger equation yields a more accurate description for a wide range of momenta, since we only had to make a restriction on the validity of the approximation for large times. For the method of averaging, on the other hand, we had to restrict ourselves to momenta close to the resonances. However, in the latter case we get a better long-time behavior.

6. Experimental requirements

In this section we rewrite the conditions, equations (24) and (25), for the realization of the Quantum FEL, that is the quantum parameter α and the maximal width of the momentum distribution in terms of experimental parameters. For this purpose we first transform these quantities which so far have been in the Bambini–Renieri frame (in this section denoted by a prime), into the lab frame. We then express our parameters with the help of the universal scaling introduced in [37] which allows us to compare our results with the ones of [21].

6.1. Quantum parameter

We recall from equations (6) and (23) the definition

$$\alpha = \frac{g\sqrt{n+1}}{q'^2/2m\hbar}$$

of the quantum parameter in the Bambini–Renieri frame and replace the photon number $n+1 \approx n$ by the number N_{e} of electrons. This substitution is justified in the Quantum FEL since each electron emitts at most one photon and we assume that we start from the vacuum.

Furthermore, we express α by quantities of the lab frame and arrive with the help of equation (A.5) at

$$\alpha = \gamma^2\frac{g\sqrt{N_{\mathrm{e}}}}{q^2/2m\hbar}$$

with the recoil $q \equiv \hbar(k_{\mathrm{L}} + k_{\mathrm{W}})$. Here, we have used the approximation $\gamma \approx \gamma_{\mathrm{BR}}$ valid for particles that move with a nonrelativistic velocity in the Bambini–Renieri frame.

In order to rewrite the coupling constant

$$g \equiv \frac{1}{\hbar}\frac{e^2}{m}\tilde{\mathcal{A}}_{\mathrm{W}}\mathcal{A}_{\mathrm{L}}$$

given by equation (B.7) we recall the wiggler parameter [28]

$$a_0 \equiv \frac{\sqrt{2}\,e\tilde{\mathcal{A}}_{\mathrm{W}}}{mc},$$

defined in equation (B.4) and introduce the explicit expression [23]

$$\mathcal{A}_{\mathrm{L}} \equiv \sqrt{\frac{\hbar}{2\epsilon_0\omega_{\mathrm{L}}V}}$$

for the amplitude of the vector potential of the laser field with the vacuum permittivity ϵ_0 and the quantization volume V.

Moreover, we employ the classical electron radius

$$r_{\mathrm{e}} \equiv \frac{e^2}{4\pi\epsilon_0 mc^2}$$

together with the Compton wavelength $\lambda_{\mathrm{C}} \equiv h/(mc)$ and find

$$\alpha = \frac{1}{\gamma^3}\frac{a_0\sqrt{r_{\mathrm{e}}n_{\mathrm{e}}}}{32\sqrt{\pi}}\,\frac{\lambda_{\mathrm{W}}^{5/2}}{\lambda_{\mathrm{C}}^{3/2}}. \tag{37}$$

Here, we have used the resonance condition, equation (A.1), and identified the ratio N_{e}/V as the electron density n_{e}.

Bonifacio *et al* [21] have introduced the parameter

$$\bar{\rho} \equiv \frac{\gamma mc}{\hbar k_{\mathrm{L}}}\rho_{\mathrm{FEL}} \tag{38}$$

as the important quantity governing the transition from the classical to the quantum regime, with the Pierce parameter [28, 37]

$$\rho_{\mathrm{FEL}} \equiv \frac{1}{2k_{\mathrm{W}}}\left(\frac{a_0^2e^2k_{\mathrm{W}}}{\epsilon_0mc^2}\frac{n_{\mathrm{e}}}{\gamma^3}\right)^{1/3} = \frac{\lambda_{\mathrm{W}}^{2/3}}{2\pi^{1/3}\gamma}\left(a_0^2n_{\mathrm{e}}r_{\mathrm{e}}\right)^{1/3} \tag{39}$$

in the case of an FEL with a laser wiggler.

While our quantum parameter α emerged from elementary arguments as well as asymptotic methods with the goal to find a two-level behavior for the momentum states of the electron, the parameter $\bar{\rho}$ surfaced [21] as a quantum correction in the characteristic equation for the linearized FEL dynamics. However, we now show that both parameters, that is α given by equation (23) and $\bar{\rho}$ defined by equations (38) and (39) are equivalent—at least in the quantum and in the classical limit.

Indeed, with the help of equations (37) and (39) we find the relation

$$\alpha = \frac{1}{\sqrt{2}}\,\bar{\rho}^{3/2}. \tag{40}$$

We emphasize that α scales with $\hbar^{-3/2}$, while $\bar{\rho}$ scales with $\hbar^{-1}$. Nevertheless, due to the connection equation (40) both parameters are equivalent descriptions of the two asymptotic cases, i.e. the classical regime $\alpha,\ \bar{\rho} \gg 1$ and the quantum regime $\alpha,\ \bar{\rho} \ll 1$.

6.2. Momentum width

Next we translate the condition for the maximal width of the momentum distribution, equation (25), into the lab frame. With the help of equation (A.6) we obtain the relation

$$\frac{\Delta p'}{mc} \approx \gamma^2\Delta\beta \approx \frac{\Delta\gamma}{\gamma}.$$

On the other hand, we find after using equation (A.5) and the resonance condition equation (A.1) the identity

$$\frac{q'}{mc} = 4\gamma\frac{\lambda_{\mathrm{C}}}{\lambda_{\mathrm{W}}} \tag{41}$$

and arrive at the requirement

$$\frac{\Delta\gamma}{\gamma} < 4\gamma\frac{\lambda_C}{\lambda_W} \tag{42}$$

for the energy spread of the electrons.

The choice $\lambda_W = 0.8\ \mu$m and $\gamma = 70$ leads us via equation (42) to a maximal relative energy spread of $\Delta\gamma/\gamma = 8.4 \times 10^{-4}$ which is of the same order of magnitude as the one claimed in [31, 38].

Unfortunately, these requirements differ by an order of magnitude from values currently reached in the experiment, which can be seen e.g. for FLASH at DESY where $\Delta\gamma/\gamma \approx 1 \times 10^{-3}$ [39]. Besides the outstanding experimental realization of a laser wiggler, the restriction equation (42) on the energy width of the electrons is the most difficult hurdle for a successfull experimental implementation of the Quantum FEL, at least in our one-dimensional theory.

7. Conclusions and outlook

In this article we have investigated quantum effects in the FEL dynamics. These phenomena already emerge from our elementary model based on a single electron and a single mode of the laser field. We have identified the quantum regime of the FEL as an effective two-level system for the momentum states of the electron and verified its existence with the help of an intuitive phase space argument as well as two asymptotic methods. Moreover, we have formulated two conditions, equations (24) and (25), to enter this quantum regime.

Indeed, we have first found the limitations of the classical description by comparing the typical momentum scale of the classical dynamics in phase space with the quantum mechanical recoil. The opposite direction, i.e. the transition from quantum mechanics to classical physics, could be investigated with an alternative approach using the Wigner distribution function [40]. For small recoil the equation of motion for the Wigner function then reduces to the Vlasov equation for a classcial distribution function.

In the further course of our article we have made use of conventional perturbation theory to obtain the dynamics in the short-time limit. In a certain parameter regime our analysis shows two resonances for the discrete momenta corresponding to emission and absorption, respectively. We then applied the more suitable method of averaging. In the quantum regime Rabi oscillations between the resonant momentum states occur, while the populations in the higher momentum states of the electron are suppressed. Identifying the resonant states as a ground and an excited state we have established the analogy to the conventional laser. Finally, we have discussed the possible operation of an FEL in this regime and investigated the experimental requirements to realize such a device.

The FEL in the quantum regime is analogous to the Jaynes–Cummings model, which describes a two-level atom interacting with a single mode of the quantized radiation field [27]. Hence, we can connect the Quantum FEL to the one-atom maser [23, 24] and calculate the photon statistics and the linewidth of the radiation by employing familiar concepts. These features will be discussed in a future article.

Furthermore, the ideas developed in this article serve as the foundation to generalize our elementary model to more complicated situations. On one hand, we have to include many modes of the radiation field in order to investigate [25] the spontaneous emission in the Quantum FEL. On the other hand, we have to develop a many-electron model [25], which is necessary to cover the high-gain regime of the FEL operation. These subjects will also be topics of future publications and shall enable us to establish the connection between our intuitive approach and the results obtained for the Quantum FEL by Bonifacio *et al.* [8, 21].

Acknowledgments

We thank W Becker, M Bussmann, A Debus, M Knobl, K Steiniger, S Varró and M S Zubairy for many fruitful discussions. EG is grateful to the Center for Integrated Quantum Science and Technology (IQ^{ST}) for a fellowship. WPS is thankful to Texas A&M University for a Texas A&M University Institute for Advanced Study (TIAS) Faculty Fellowship.

Appendix A. Bambini–Renieri frame

Our approach towards the FEL takes advantage of the co-moving Bambini–Renieri frame [26] where a nonrelativistic treatment of the FEL dynamics is possible. This frame of reference is defined by the condition that the wave numbers of the wiggler and the laser field coincide. Thus the electrons interact with a standing light field.

In this appendix we summarize the transformation properties of quantities, such as the wave vectors of the fields or the momentum of the electron, when we go from the laboratory to the Bambini–Renieri frame. This discussion gives us the chance to express the parameters crucial for the operation of the Quantum FEL discussed in section 6 in terms of the laboratory frame.

In [41] it was suggested to use for the Quantum FEL a laser wiggler instead of a magnetostatic wiggler. Hence, we treat the wiggler as an optical undulator, i.e. an electromagnetic wave propagating towards the electron. The possible implementation of such a laser wiggler was e.g. discussed in [42–44].

In the Bambini–Renieri frame there is no difference between a magnetostatic or an optical undulator, because both are described by a wave with the same wave number k as the laser field. However, there is of course a difference in the lab frame, which is best seen for the classical resonance condition.

Indeed, when we want to determine the wavelength $\lambda'_{\mathrm{W}} \equiv \lambda'$ of the (laser) wiggler in the rest frame of the electron we have to apply the Doppler shift and arrive at the transformed wavelength $\lambda' \approx \lambda_{\mathrm{W}}/2\gamma$. Here we have introduced the wavelength λ_{W} of the wiggler in the lab frame and the relativistic factor γ which is given by the ratio of the kinetic energy of the electron to its rest energy.

The electrons are basically dipoles radiating at the wavelength $\lambda' = \lambda'_{\mathrm{L}}$ of their excitation. Returning to the lab frame by a second Doppler shift we find the expression [13]

$$\lambda_{\mathrm{L}} = \frac{\lambda_{\mathrm{W}}}{4\gamma^2} \tag{A.1}$$

for the wavelength of the laser. We observe [28] that it differs from the magnetostatic case by a factor of $1/2$. The reason for this deviation lies in the fact that the first Doppler shift has to be replaced by the Lorentz contraction $\lambda' = \lambda_{\mathrm{W}}/\gamma$ of the periodicity λ_{W} of the wiggler.

We start in the lab frame I and transform into an inertial frame I' moving with $v = \beta c$ along the z-axis. A helpful quantity for these calculations is the four-velocity u^μ. An observer at rest in the co-moving frame possesses the four-velocity

$$\left(u'\right)^\mu \equiv c\,(1,\,0,\,0,\,0),$$

while his four-velocity in the lab frame reads

$$u^\mu \equiv \gamma c\,(1,\,0,\,0,\,\beta),$$

and the relativistic factor γ takes the form

$$\gamma \equiv \frac{1}{\sqrt{1-\beta^2}}. \tag{A.2}$$

The four-wave vectors of the laser and the wiggler field in the laboratory frame are given by

$$k_{\mathrm{L}}^\mu \equiv k_{\mathrm{L}}\,(1,\,0,\,0,\,1),$$

and

$$k_{\mathrm{W}}^\mu \equiv k_{\mathrm{W}}\,(1,\,0,\,0,\,-1),$$

where we have defined the wave numbers of the laser field $k_{\mathrm{L}} \equiv 2\pi/\lambda_{\mathrm{L}}$ and of the wiggler $k_{\mathrm{W}} \equiv 2\pi/\lambda_{\mathrm{W}}$ and we have used the dispersion relations $\omega_{\mathrm{L}} = ck_{\mathrm{L}}$ and $\omega_{\mathrm{W}} = ck_{\mathrm{W}}$ for the frequencies ω_{L} and ω_{W} in the zeroth components of the four-vectors.

Note that the laser field is travelling in the positive z-direction, while the wiggler field propagates in the negative z-direction which is apparent from the different signs in the last component of the four-vectors. When transforming into the Bambini–Renieri frame only the wave numbers change and per definition they have to be equal in this particular frame of reference , i.e. $k'_{\mathrm{L}} = k'_{\mathrm{W}} \equiv k'$.

A Lorentz transformation leaves a scalar product of two four-vectors invariant. Since the scalar product $((k'_{\mathrm{L}})^\mu - (k'_{\mathrm{W}})^\mu)\,u'_\mu$ vanishes in the co-moving frame the same expression $(k_{\mathrm{L}}^\mu - k_{\mathrm{W}}^\mu)\,u_\mu$ in the lab frame has to be zero as well. From this condition we find the expression

$$\beta_{\mathrm{BR}} = \frac{k_{\mathrm{L}} - k_{\mathrm{W}}}{k_{\mathrm{L}} + k_{\mathrm{W}}} \tag{A.3}$$

for the scaled velocity of the Bambini–Renieri frame relative to the lab frame.

With the help of the definition, equation (A.2), we obtain

$$\gamma_{\mathrm{BR}} = \frac{k_{\mathrm{L}} + k_{\mathrm{W}}}{2\sqrt{k_{\mathrm{L}}k_{\mathrm{W}}}} \tag{A.4}$$

for the relativistic factor γ_{BR}.

After equating $((k'_{\mathrm{L}})^\mu + (k'_{\mathrm{W}})^\mu)\,u'_\mu$ with $(k_{\mathrm{L}}^\mu + k_{\mathrm{W}}^\mu)\,u_\mu$ and inserting the expressions equation (A.3) for β_{BR} and equation (A.4) for γ_{BR} we arrive at

$$k' = \sqrt{k_{\mathrm{L}} k_{\mathrm{W}}} = \frac{1}{2\gamma_{\mathrm{BR}}}(k_{\mathrm{L}} + k_{\mathrm{W}}) \tag{A.5}$$

for the transformed wave number.

Another important quantity in our analysis of the Quantum FEL is the momentum p' of a particle with mass m travelling along the z-axis. Therefore, we introduce the four-momentum $p^{\mu} \equiv mcu^{\mu}$. After equating the scalar product $p_{\mu}(k_{\mathrm{L}}^{\mu} - k_{\mathrm{W}}^{\mu})$ in both frames of reference we obtain the transformed momentum

$$p' = \gamma_{\mathrm{BR}} p - \gamma p_{\mathrm{BR}} = \gamma\gamma_{\mathrm{BR}} mc(\beta - \beta_{\mathrm{BR}}) \tag{A.6}$$

where p is the momentum of the particle in the lab frame and $p_{\mathrm{BR}} \equiv \gamma_{\mathrm{BR}} mc\ \beta_{\mathrm{BR}}$ is the one corresponding to a particle at rest in the Bambini–Renieri frame.

We conclude by mentioning that we omit in the main body of this article the primes for quantities in the Bambini–Renieri frame, unless we compare them with the ones in the lab frame.

Appendix B. Derivation of the Hamiltonian

In this appendix we derive the Hamiltonian, equation (4), used in the main body of this article to describe the nonrelativistic quantum theory of the FEL in the Bambini–Renieri frame summarized in appendix A. We first obtain the classical Hamiltonian and then quantize it.

B.1. Taking the square root

We start from the relativistic Hamiltonian [45]

$$H(\boldsymbol{r}, \boldsymbol{p}, t) \equiv c\sqrt{(\boldsymbol{p} - e\boldsymbol{A}(\boldsymbol{r}, t))^2 + m_0^2 c^2} \tag{B.1}$$

of a single electron with the rest mass m_0 of the electron, the elementary charge e interacting at the position $\boldsymbol{r}$ and with the momentum $\boldsymbol{p}$ with an electromagnetic field. This field is given by the vector potential $\boldsymbol{A} \equiv \boldsymbol{A}_{\mathrm{L}} + \boldsymbol{A}_{\mathrm{W}}$ consisting of the laser field (subscript L)

$$\boldsymbol{A}_{\mathrm{L}}(z, t) \equiv \tilde{\mathcal{A}}_{\mathrm{L}}\ \boldsymbol{\epsilon}\ \mathrm{e}^{-\mathrm{i}k_{\mathrm{L}}(ct-z)} + \mathrm{c.c.} \tag{B.2}$$

travelling in positive z-direction and the wiggler (subscript W)

$$\boldsymbol{A}_{\mathrm{W}}(z, t) \equiv \tilde{\mathcal{A}}_{\mathrm{W}}\ \boldsymbol{\epsilon}\ \mathrm{e}^{-\mathrm{i}k_{\mathrm{W}}(ct+z)} + \mathrm{c.c.} \tag{B.3}$$

which propagates in the opposite direction as apparent from the opposite signs of the phases. The amplitudes of the vector potentials are given by $\tilde{\mathcal{A}}_{\mathrm{L}}$ and $\tilde{\mathcal{A}}_{\mathrm{W}}$, and the corresponding wave numbers k_{L} and k_{W} coincide in the Bambini–Renieri frame, i.e. $k_{\mathrm{L}} = k_{\mathrm{W}} \equiv k$. The polarizations of both fields are chosen to be circular with the polarization vector $\boldsymbol{\epsilon}$ fulfilling the relations $\boldsymbol{\epsilon}^2 = \boldsymbol{\epsilon}^{*2} = 0$ and $\boldsymbol{\epsilon} \cdot \boldsymbol{\epsilon}^* = 1$. Using Coulomb gauge, i. e. $\boldsymbol{\nabla} \cdot \boldsymbol{A} = 0$, the polarization vectors are orthognal to the z-direction.

Under these assumptions the Hamiltonian is independent of the x and y coordinate and we can infer that the conjugate momenta are constants of motion which even vanish if we choose the initial momentum parallel to the z-direction. Thus, only the z-coordinate and its conjugate momentum $p_z \equiv p$ are dynamical variables for the electron. Moreover, the scalar product $\boldsymbol{p} \cdot \boldsymbol{A}$ vanishes for transversal fields and the Hamiltonian, equation (B.1) takes the form

$$H(z, p, t) = c\sqrt{p^2 + 2e^2 \boldsymbol{A}_{\mathrm{L}}(z, t) \cdot \boldsymbol{A}_{\mathrm{W}}(z, t) + m^2 c^2}$$

with the shifted mass

$$m^2 \equiv m_0^2\left(1 + a_0^2\right).$$

Here we have introduced the wiggler parameter [28]

$$a_0 \equiv \frac{\sqrt{2}\, e\left|\tilde{\mathcal{A}}_{\mathrm{W}}\right|}{m_0 c} \tag{B.4}$$

and have neglected the contribution arising from $\boldsymbol{A}_{\mathrm{L}}^2$, since $|\tilde{\mathcal{A}}_{\mathrm{L}}| \ll |\tilde{\mathcal{A}}_{\mathrm{W}}|$.

Next, we perform the nonrelativistic approximation by expanding the relativistic square root

$$H(z, p, t) = mc^2\sqrt{1 + \left(\frac{p}{mc}\right)^2 + \frac{2e^2}{(mc)^2}\, \boldsymbol{A}_{\mathrm{L}}(z, t) \cdot \boldsymbol{A}_{\mathrm{W}}(z, t)}$$

which yields

$$H(z,\,p,\,t) \approx mc^2 + \frac{p^2}{2m} + \frac{e^2}{m}\boldsymbol{A}_{\mathrm{L}}(z,\,t)\cdot\boldsymbol{A}_{\mathrm{W}}(z,\,t). \tag{B.5}$$

This expansion is only valid if the momentum p of the electron is nonrelativistic for all times, i.e. $p \ll mc$. For the classical FEL the variable p assumes its maximal value $\sqrt{2mV_0} = \sqrt{2e^2\tilde{\mathcal{A}}_{\mathrm{L}}\tilde{\mathcal{A}}_{\mathrm{W}}}$ with the constraint that the electron performs a bounded motion [28]; for all reasonable parameters $e^2|\tilde{\mathcal{A}}_{\mathrm{L}}||\tilde{\mathcal{A}}_{\mathrm{W}}|/(m^2c^2) \ll 1$ and the motion in the Bambini–Renieri frame is nonrelativistic.

In the main body of this article we show that in the quantum regime the change of the electron momentum is of the order of the recoil $q \equiv 2\hbar k$, which translates with the help of equation (41) to $q/mc = 4\gamma\lambda_{\mathrm{C}}/\lambda_{\mathrm{W}} \ll 1$ and ensures the validity of the approximate Hamiltonian, equation (B.5), for the Quantum FEL, too.

After inserting the explicit expressions for the vector potentials, equations (B.2) and (B.3), we arrive at

$$H(z,\,p) = \frac{p^2}{2m} + \frac{e^2}{m}\tilde{\mathcal{A}}_{\mathrm{W}}\left(\tilde{\mathcal{A}}_{\mathrm{L}}\mathrm{e}^{+\mathrm{i}2kz} + \mathrm{c.c.}\right), \tag{B.6}$$

where we have neglected the constant term mc^2. We emphasize that this Hamiltonian is time-independent, since the time-dependent phases cancel in the Bambini–Renieri frame with our particular choice of polarization.

B.2. Quantization

We proceed by deriving the quantized version of the Hamiltonian, equation (B.6). First, we quantize the motion of the electron by replacing its position z and conjugate momentum p by their operator counterparts $\hat{z}$ and $\hat{p}$ fulfilling the commutation relation $[\hat{z},\,\hat{p}] = \mathrm{i}\hbar$. Furthermore, we treat the laser field as a quantized field and introduce the photon annihilation $\hat{a}_{\mathrm{L}}$ and creation operator $\hat{a}_{\mathrm{L}}^{\dagger}$ with the bosonic commutation relation $[\hat{a}_{\mathrm{L}},\,\hat{a}_{\mathrm{L}}^{\dagger}] = 1$ via the substitutions

$$\tilde{\mathcal{A}}_{\mathrm{L}} \rightarrow \mathcal{A}_{\mathrm{L}}\,\hat{a}_{\mathrm{L}}$$

and

$$\tilde{\mathcal{A}}_{\mathrm{L}}^{*} \rightarrow \mathcal{A}_{\mathrm{L}}\,\hat{a}^{\dagger}.$$

Here $\mathcal{A}_{\mathrm{L}}$ denotes the amplitude of the quantized laser field.

We emphasize that this quantized version of the vector potential is not in the Schrödinger picture, where the fundamental operators have to be time-independent. This feature originates from the fact that we have already time-dependent fields in the classical Hamiltonian (B.1) instead of time-independent ones and an additional free Hamiltonian of the electromagnetic field.

Due to its high intensity we treat the wiggler as a classical, external field with $\tilde{\mathcal{A}}_{\mathrm{W}}^{*} = \tilde{\mathcal{A}}_{\mathrm{W}}$=const. The mechanical action of the wiggler field is taken into account by the position operator $\hat{z}$ of the electron in equation (B.3).

Thus, we arrive at the quantized Hamiltonian

$$\hat{H}' = \frac{\hat{p}^2}{2m} + \hbar g\left(\hat{a}_{\mathrm{L}}\,\mathrm{e}^{+2\mathrm{i}k\hat{z}} + \hat{a}_{\mathrm{L}}^{\dagger}\,\mathrm{e}^{-2\mathrm{i}k\hat{z}}\right),$$

where we have have defined the coupling constant

$$g \equiv \frac{1}{\hbar}\frac{e^2}{m}\mathcal{A}_{\mathrm{L}}\tilde{\mathcal{A}}_{\mathrm{W}}. \tag{B.7}$$

This Hamiltonian already shows us the basic processes in the FEL: if a photon is created by $\hat{a}_{\mathrm{L}}^{\dagger}$, the electron decelerates by the recoil $q \equiv 2\hbar k$, symbolized by the momentum shift operator $\mathrm{e}^{-\mathrm{i}2k\hat{z}}$. In the case of absorption, $\hat{a}_{\mathrm{L}}$, the electron gains momentum, denoted by the different sign in the phase of the momentum shift operator.

Appendix C. Short-time expansion: second-order contribution

In this appendix we derive explicit expressions for the coefficients $c_{\mu}(p;\,t)$ defined in equation (13) from the expansion in equation (10) including second-order processes. For this purpose, we calculate the matrix element $\mathcal{M} \equiv \langle n+\mu,\,p-\mu q|\,\hat{\mathcal{U}}_2\,|\psi(0)\rangle$ and find from equation (11) with the definition of the second-order contribution

$$\mathcal{M} = -\frac{\mathrm{i}}{\hbar}\int_0^t \mathrm{d}t_2 \langle n+\mu,\, p-\mu q|\, \hat{H}(t_2)\hat{\mathcal{U}}_\mathrm{I}(t_2)|\psi(0)\rangle.$$

The first integration has already been performed in the context of the first-order expansion in equation (14) and we use these results to obtain the expression

$$\begin{aligned}\mathcal{M} = &\left[(n+\mu)\,\mathcal{I}_0^{(-)} + (n+\mu+1)\,\mathcal{I}_0^{(+)}\right]c_\mu(0) + \sqrt{n+\mu}\,\sqrt{n+\mu-1}\,\mathcal{I}_{-2}\,c_{\mu-2}(0)\\ &+ \sqrt{n+\mu+2}\,\sqrt{n+\mu+1}\,\mathcal{I}_{+2}\,c_{\mu+2}(0)\end{aligned} \tag{C.1}$$

describing the two-photon processes.

In equation (C.1) we have defined the integrals

$$\mathcal{I}_{\pm 2} \equiv -\int_0^t \mathrm{d}t_2\, g^2 t_2 \mathrm{e}^{\pm\mathrm{i}\left(3\frac{p}{q}\mp\frac{5}{2}\right)\omega_\mathrm{r} t_2}\mathrm{sinc}\left(\frac{\Delta_{\frac{\pm 3-1}{2}}t_2}{2}\right)$$

and

$$\mathcal{I}_0^{(\pm)} \equiv -\int_0^t \mathrm{d}t_2\, g^2 t_2 \mathrm{e}^{\pm\mathrm{i}\Delta_{\frac{-1\pm 2}{2}}t_2}\mathrm{sinc}\left(\frac{\Delta_{\frac{-1\pm 1}{2}}t_2}{2}\right)$$

where we have recalled from equation (7) the definition

$$\Delta_j = \Delta_j(p) \equiv 2\omega_\mathrm{r}\left(\frac{p}{q} - \frac{1}{2} - j\right)$$

of the detuning to simplify the notation.

Next we perform the remaining integration and arrive at the explicit expressions

$$\mathcal{I}_{+2} \equiv -\mathrm{i}\frac{(gt)^2}{\Delta_1 t/2}\left[\mathrm{e}^{\mathrm{i}\frac{\Delta_0 t}{2}}\mathrm{sinc}\left(\frac{\Delta_0 t}{2}\right) - \mathrm{e}^{\mathrm{i}\Delta_{\frac{1}{2}}t}\mathrm{sinc}\left(\Delta_{\frac{1}{2}}t\right)\right] \tag{C.2}$$

and

$$\mathcal{I}_{-2} \equiv -\mathrm{i}\frac{(gt)^2}{\Delta_{-2} t/2}\left[\mathrm{e}^{-\mathrm{i}\Delta_{-\frac{3}{2}}t}\mathrm{sinc}\left(\Delta_{-\frac{3}{2}}t\right) - \mathrm{e}^{-\mathrm{i}\frac{\Delta_{-1}t}{2}}\mathrm{sinc}\left(\frac{\Delta_{-1}t}{2}\right)\right] \tag{C.3}$$

for the coefficients of the two-photon transitions.

The corrections to $c_\mu(p;\, t=0)$ that arise from two-photon processes take the form

$$\mathcal{I}_0^{(+)} = -\mathrm{i}\frac{(gt)^2}{\Delta_0 t/2}\left[\mathrm{e}^{\mathrm{i}\frac{\Delta_1 t}{4}}\mathrm{sinc}\left(\frac{\Delta_1 t}{4}\right) - \mathrm{e}^{\mathrm{i}\frac{2\Delta_0+\Delta_1}{4}t}\mathrm{sinc}\left(\frac{2\Delta_0+\Delta_1}{4}t\right)\right]$$

and

$$\mathcal{I}_0^{(-)} = -\mathrm{i}\frac{(gt)^2}{\Delta_{-1} t/2}\left[\mathrm{e}^{-\mathrm{i}\frac{2\Delta_{-1}+\Delta_{-2}}{4}t}\mathrm{sinc}\left(\frac{2\Delta_{-1}+\Delta_{-2}}{4}t\right) - \mathrm{e}^{-\mathrm{i}\frac{\Delta_{-2}t}{4}}\mathrm{sinc}\left(\frac{\Delta_{-2}t}{4}\right)\right].$$

This representation shows that these contributions only occur in the second-order expansion since they are proportional to $(g\sqrt{n+1}\,t)^2$.

In the main part of our article we analyze the transition probabilities for the two-photon transitions starting from an initial Fock state $|n\rangle$ for the laser field and the momentum distribution $\phi(p)$ for the electron. Hence, we choose the initial condition $c_\mu(0) \equiv \delta_{\mu,0}\phi(p)$, which leads us to

$$c_{+2}(t) = -\mathrm{i}g\sqrt{n+2}\;t\;\frac{g\sqrt{n+1}}{\omega_\mathrm{r}}\,\mathcal{E}_{+2}\,\phi(p) \tag{C.4}$$

with the dimensionless momentum-dependent amplitude

$$\mathcal{E}_{+2} \equiv \frac{\mathrm{e}^{-\mathrm{i}\Delta_{\frac{1}{2}}t}}{\left(\frac{p}{q}-\frac{1}{2}\right)}\mathrm{sinc}\left(\Delta_{\frac{1}{2}}t\right) - \frac{\mathrm{e}^{-\mathrm{i}\frac{\Delta_1 t}{2}}}{\left(\frac{p}{q}-\frac{1}{2}\right)}\mathrm{sinc}\left(\frac{\Delta_1 t}{2}\right).$$

Here we have shifted the momentum by $-2q$ leading to a shift of 2 in the index of the detunings Δ_j in equation (C.2).

Similarly, the loss of two photons follows from the relation

$$c_{-2}(t) = -\mathrm{i}g\sqrt{n}\; t\; \frac{g\sqrt{n-1}}{\omega_\mathrm{r}}\; \mathcal{E}_{-2}\; \phi(p), \tag{C.5}$$

with the dimensionless amplitude

$$\mathcal{E}_{-2} \equiv \frac{\mathrm{e}^{\mathrm{i}\frac{\Delta_{-2}t}{2}}}{\left(\frac{p}{q}+\frac{1}{2}\right)}\mathrm{sinc}\left(\frac{\Delta_{-2}t}{2}\right) - \frac{\mathrm{e}^{\mathrm{i}\Delta_{-\frac{3}{2}}t}}{\left(\frac{p}{q}+\frac{1}{2}\right)}\mathrm{sinc}\left(\Delta_{-\frac{3}{2}}t\right),$$

where now the indices of the detunings Δ_j in equation (C.3) are shifted by -2 corresponding to a shift in momentum of $+2q$.

To obtain the probability densitites for the corresponding processes, we have to take the modulus square of equations (C.4) and (C.5), respectively, and we find the expressions

$$\left|c_{+2}(p;\,t)\right|^2 = g^2(n+2)t^2\left(\frac{g\sqrt{n+1}}{\omega_\mathrm{r}}\right)^2\left|\mathcal{E}_{+2}\right|^2|\phi(p)|^2$$

and

$$\left|c_{-2}(p;\,t)\right|^2 = g^2(n-1)t^2\left(\frac{g\sqrt{n}}{\omega_\mathrm{r}}\right)^2\left|\mathcal{E}_{-2}\right|^2|\phi(p)|^2,$$

discussed in detail in section 4.2.

Appendix D. The method of averaging applied to the FEL

In this appendix we show the detailed calculations that lead to the results of section 5 which allow us to identify the Quantum FEL as a two-level system. In particular, we derive within the framework of the method of averaging [22, 46] the probabilities for the electron to be in the momentum states $\mu = 0$ and $\mu = -1$. For the sake of simplicity we restrict ourselves to the case of the resonance $p = q/2$.

D.1. Basic elements

To keep our article self-contained we first explain the basic elements of the method of averaging before we consider the specific situation of the FEL dynamics. Since here we are following rather closely the approach of [34] we only sketch the main ideas of the technique and refer the interested reader to this article for details.

We start by expanding the probability amplitudes

$$\boldsymbol{c}(t) = \boldsymbol{\sigma}(t) + \varepsilon\boldsymbol{f}_1(t) + \varepsilon^2\boldsymbol{f}_2(t) + \cdots$$

into a power series in ε, where we have separated $\boldsymbol{c}(t)$ into a slowly-varying part $\boldsymbol{\sigma}(t)$ and rapidly-oscillating parts $\boldsymbol{f}_j(t)$ which are suppressed by powers of ε.

In the second step we assume that $\boldsymbol{f}_j$ are linear functions of $\boldsymbol{\sigma}$, i.e. $\boldsymbol{f}_j = \mathcal{F}_j\boldsymbol{\sigma}$, yielding

$$\boldsymbol{c}(t) = \left(\mathbb{1} + \varepsilon\mathcal{F}_1(t) + \varepsilon^2\mathcal{F}_2(t) + \cdots\right)\boldsymbol{\sigma}(t). \tag{D.1}$$

Moreover, we assume for the slowly- varying coefficients $\boldsymbol{\sigma}(t)$ the effective Schrödinger equation

$$\mathrm{i}\dot{\boldsymbol{\sigma}}(t) = \left(\varepsilon\mathcal{H}_0 + \varepsilon^2\mathcal{P}_2 + \epsilon^3\mathcal{P}_3 + \cdots\right)\boldsymbol{\sigma}(t) \tag{D.2}$$

with the higher-order contributions $\mathcal{P}_j$ to the effective, time-independent Hamiltonian.

Based on these assumptions we now have to determine $\mathcal{P}_j$ and $\mathcal{F}_j(t)$. We achieve this goal by inserting equation (D.1) into the Schrödinger equation, equation (27), for the coefficients $\boldsymbol{c}(t)$ using equation (D.2) and solving the resulting equations order by order. The main difference between the method of averaging and ordinary perturbative methods is that we absorb the time-independent terms into $\mathcal{P}_j$ to avoid secular growth [46].

In the first steps of our calculation we subsequently obtain

$$\mathcal{F}_1(t) = -\sum_{\nu\neq 0}\frac{\mathrm{e}^{\mathrm{i}\nu\omega_\mathrm{r}t}}{\nu\omega_\mathrm{r}}\,\mathcal{H}_\nu$$

and

$$\mathcal{P}_2 = -\sum_{\nu\neq 0}\frac{\mathcal{H}_{-\nu}\mathcal{H}_\nu}{\nu\omega_\mathrm{r}} \tag{D.3}$$

for the lowest-order corrections.

In the same manner—but with more involved calculations—we arrive at

$$\mathcal{F}_2(t) = -\sum_{\lambda\neq 0}\frac{\mathrm{e}^{\mathrm{i}\lambda\omega_\mathrm{r}t}}{\lambda^2\omega_\mathrm{r}^2}\,[\mathcal{H}_\lambda,\,\mathcal{H}_0] + \sum_{\substack{\nu,\mu\neq 0\\ \nu-\mu\neq 0}}\frac{\mathrm{e}^{\mathrm{i}\nu\omega_\mathrm{r}t}}{\nu\mu\omega_\mathrm{r}^2}\,\mathcal{H}_{\nu-\mu}\mathcal{H}_\mu \tag{D.4}$$

and

$$\mathcal{P}_3 = -\sum_{\lambda\neq 0}\frac{1}{\lambda^2\omega_\mathrm{r}^2}\,\mathcal{H}_\lambda[\mathcal{H}_{-\lambda},\,\mathcal{H}_0] + \sum_{\substack{\mu,\nu\neq 0\\ \mu+\nu\neq 0}}\frac{\mathcal{H}_{-\mu-\nu}\mathcal{H}_\nu\mathcal{H}_\mu}{\mu(\mu+\nu)\omega_\mathrm{r}^2},$$

which give the next higher orders for the rapidly varying part and for the slowly varying part, respectively.

D.2. Application to Quantum FEL

Having developed the mathematical tools we can now consider our problem of interest, i.e. the FEL dynamics. Therefore, we first have to look at the initial conditions: at $t = 0$ the electron should be at the momentum eigenstate with $p = q/2$ which translates into the initial condition $c_\mu(t = 0) = \delta_{\mu,0}$ for the probability amplitudes. However, we do not know yet the initial conditions for the slowly-varying contributions $\boldsymbol{\sigma}(0)$. We find them by inverting equation (D.1), that is

$$\boldsymbol{\sigma}(0) = \left(\mathbb{1} + \varepsilon\mathcal{F}_1(0) + \varepsilon^2\mathcal{F}_2(0)\right)^{-1}\boldsymbol{c}(0)$$

or

$$\boldsymbol{\sigma}(0) = \left(\mathbb{1} - \varepsilon\mathcal{F}_1(0) + \varepsilon^2\mathcal{F}_1^2(0) - \varepsilon^2\mathcal{F}_2(0)\right)\boldsymbol{c}(0) + \mathcal{O}\left(\varepsilon^3\right), \tag{D.5}$$

where we have only kept terms up to the order ε^2.

To simplify our notation we restrict ourselves to the states from $\mu = -1$ to $\mu = 2$ and introduce the notation $\boldsymbol{\sigma} \equiv (\sigma_{-1},\,\sigma_0,\,\sigma_1,\,\sigma_2)^\mathrm{T}$. Other contributions do not play a role if we are only interested in the lowest-order corrections. From equation (D.5) we obtain

$$\boldsymbol{\sigma}(0) = \left(\frac{\alpha}{2},\,1-\frac{\alpha^2}{4},\,0,\,\frac{\alpha^2}{4}\right)^\mathrm{T}, \tag{D.6}$$

where we have used the approximation $\sqrt{n\pm 2} \approx \sqrt{n\pm 1} \approx \sqrt{n}$ valid for $n \gg 1$ to introduce the quantum parameter α defined in equation (23) as the expansion parameter of our approach.

With the help of equations (D.3) and (D.4) we arrive at the linear differential equation

$$\mathrm{i}\dot{\boldsymbol{\sigma}}(t) = \omega_\mathrm{r}\begin{pmatrix} \frac{\alpha^2}{4} & 0 & 0 & \frac{\alpha^3}{4}\\ 0 & -\frac{\alpha^2}{2} & \alpha\left(1-\frac{\alpha^2}{4}\right) & 0\\ 0 & \alpha\left(1-\frac{\alpha^2}{4}\right) & -\frac{\alpha^2}{2} & 0\\ \frac{\alpha^3}{4} & 0 & 0 & \frac{\alpha^2}{4}\end{pmatrix}\boldsymbol{\sigma}(t), \tag{D.7}$$

which we have to solve subjected to the initial condition equation (D.6).

We notice that the states with $\mu = 0$ and $\mu = 1$, as well as the states $\mu = -1$ and $\mu = 2$ couple separately so that we effectively have to solve two two-dimensional problems. Furthermore when we keep track of the contributions of this equation, we realize that all diagonal terms arise from $\mathcal{P}_2$. Hence, to obtain the first corrections to the Rabi frequency $\alpha\omega_\mathrm{r}$ of the two-level system with $\mu = 0$ and $\mu = 1$, and to include the first off-diagonal contributions for the coupled states $\mu = -1$ and $\mu = 2$ we have to keep the next higher order term $\mathcal{P}_3$ of the effective Hamiltonian.

The solution of equation (D.7) reads

$$\boldsymbol{\sigma}(t) = \mathrm{e}^{\mathrm{i}\alpha^2\omega_\mathrm{r}t/2}\left(1-\frac{\alpha^2}{4}\right)\begin{pmatrix}0\\ \cos\left[\alpha\left(1-\frac{\alpha^2}{4}\right)\omega_\mathrm{r}t\right]\\ -\mathrm{i}\sin\left[\alpha\left(1-\frac{\alpha^2}{4}\right)\omega_\mathrm{r}t\right]\\ 0\end{pmatrix} + \mathrm{e}^{-\mathrm{i}\alpha^2\omega_\mathrm{r}t/4}\,\frac{\alpha}{2}\left(1+\frac{\alpha}{2}\right)\begin{pmatrix}\cos\left(\frac{\alpha^3}{4}\omega_\mathrm{r}t\right)\\ 0\\ 0\\ -\mathrm{i}\sin\left(\frac{\alpha^3}{4}\omega_\mathrm{r}t\right)\end{pmatrix}.$$

Finally, we use equation (D.1) to obtain the coefficients $\boldsymbol{c}(t)$ leading us to the transition probabilities for the excited state

$$|c_0(t)|^2 = \left(1 - \frac{\alpha^2}{2}\right)\cos^2\left[\alpha\left(1 - \frac{\alpha^2}{4}\right)\omega_r t\right] + \frac{\alpha^2}{2}\cos\left(\frac{\alpha^3}{4}\omega_r t\right)\cos\left[\left(1 + \frac{3\alpha^2}{8}\right)2\omega_r t\right]\cos\left[\alpha\left(1 - \frac{\alpha^2}{4}\right)\omega_r t\right], \quad (D.8)$$

the ground state

$$|c_1(t)|^2 = \left(1 - \frac{\alpha^2}{2}\right)\sin^2\left[\alpha\left(1 - \frac{\alpha^2}{4}\right)\omega_r t\right] + \frac{\alpha^2}{2}\sin\left(\frac{\alpha^3}{4}\omega_r t\right)\cos\left[\left(1 + \frac{3\alpha^2}{8}\right)2\omega_r t\right]\sin\left[\alpha\left(1 - \frac{\alpha^2}{4}\right)\omega_r t\right],$$

and the neighboring levels

$$|c_{-1}(t)|^2 = \frac{\alpha^2}{4}\left(\cos^2\left(\frac{\alpha^3}{4}\omega_r t\right) + \cos^2\left[\alpha\left(1 - \frac{\alpha^2}{4}\right)\omega_r t\right] - 2\cos\left(\frac{\alpha^3}{4}\omega_r t\right)\cos\left[\left(1 + \frac{3\alpha^2}{8}\right)2\omega_r t\right]\cos\left[\alpha\left(1 - \frac{\alpha^2}{4}\right)\omega_r t\right]\right),$$

and

$$|c_2(t)|^2 = \frac{\alpha^2}{4}\left(\sin^2\left(\frac{\alpha^3}{4}\omega_r t\right) + \sin^2\left[\alpha\left(1 - \frac{\alpha^2}{4}\right)\omega_r t\right] - 2\sin\left(\frac{\alpha^3}{4}\omega_r t\right)\cos\left[\left(1 + \frac{3\alpha^2}{8}\right)2\omega_r t\right]\sin\left[\alpha\left(1 - \frac{\alpha^2}{4}\right)\omega_r t\right]\right). \quad (D.9)$$

Here, we have kept terms in the amplitude up to second order in α, while we have calculated the contributions in the phases up to third order in α, as to obtain the lowest-order corrections to the two-level approximation given by equation (33).

References

[1] Fedorov M V 1981 *Prog. Quantum Electron.* **7** 73–116
Becker W and McIver J K 1983 *J. Phys. Colloq.* **44** C1 289–311
Friedman A, Gover A, Kurizki G, Ruschin S and Yariv A 1988 *Rev. Mod. Phys.* **60** 471–535
[2] Hopf F A, Meystre P, Scully M O and Louisell W H 1976 *Opt. Commun.* **18** 413–6
[3] Colson W B 1977 *Phys. Lett.* A **64** 190–2
[4] Moore G T and Scully M O 1980 *Phys. Rev.* A **21** 2000–8
Bonifacio R, Meystre P, Moore G T and Scully M O 1980 *Phys. Rev.* A **21** 2009–19
[5] Emma P *et al* 2010 *Nat. Photonics* **4** 641–7
[6] Decking W and Le Pimpec F 2014 *Proc. 36th Free-Electron Laser Conf.* (*Basel, Switzerland*) pp 623–8
[7] Bonifacio R, Piovella N and Robb G R M 2009 *Fortschr. Phys.* **57** 1041–51
[8] Bonifacio R, Piovella N and Robb G R M 2005 *Nucl. Instrum. Methods Phys. Res.* A **543** 645–52
[9] Pantell R H, Soncini G and Puthoff H E 1968 *IEEE J. Quantum Electron.* **4** 905–7
Madey J M J 1971 *J. Appl. Phys.* **42** 1906–13
Sukhatme V P and Wolff P A 1973 *J. Appl. Phys.* **44** 2331–4
[10] Borenstein M and Lamb W E 1972 *Phys. Rev.* A **5** 1298–311
[11] Becker W and Mitter H 1979 *Z. Phys. B: Condens. Matter* **35** 399–404
[12] McIver J K and Fedorov M V 1979 *J. Exp. Theor. Phys.* **49** 1012–9
[13] Fedorov M V 1997 *Atomic and Free Electrons in a Strong Light Field* (Singapore: World Scientific)
[14] Becker W 1980 *Z. Phys. B: Condens. Matter* **38** 287–92
Becker W 1980 *Opt. Commun.* **33** 69–74
Becker W and McIver J K 1983 *Phys. Rev.* A **27** 1030–43
Becker W and McIver J K 1987 *Phys. Rep.* **154** 205–45
[15] Ciocci F, Dattoli G, Renieri A and Torre A 1986 *Phys. Rep.* **141** 1–50
[16] Becker W and Zubairy M S 1982 *Phys. Rev.* A **25** 2200–7
Becker W, Scully M O and Zubairy M S 1982 *Phys. Rev. Lett.* **48** 475–7
Becker W, Scully M O and Zubairy M S 1984 *Coherence and Quantum Optics: V* (New York: Plenum)
Becker W, Gea-Banacloche J and Scully M O 1986 *Phys. Rev.* A **33** 2174–6
[17] Gea-Banacloche J 1985 *Phys. Rev.* A **31** 1607–21
[18] Orszag M 1984 *Opt. Acta: Int. J. Opt.* **31** 267–70
Orszag M and Ramirez R 1986 *J. Opt. Soc. Am.* B **3** 895–900
[19] Schroeder C B, Pellegrini C and Chen P 2001 *Phys. Rev.* E **64** 056502
[20] Bonifacio R, Pellegrini C and Narducci L M 1984 *Opt. Commun.* **50** 373–8
[21] Bonifacio R, Piovella N, Robb G R M and Schiavi A 2006 *Phys. Rev. Spec. Top.—Accelerators Beams* **9** 090701
[22] Bogoliubov N N and Mitropolsky Y A 1961 *Asymptotic Methods in the Theory of Non-Linear Oscillations* (Delhi: Hindustan)

[23] Schleich W P 2001 *Quantum Optics in Phase Space* (Weinheim: Wiley-VCH)
[24] Meschede D, Walther H and Müller G 1985 *Phys. Rev. Lett.* **54** 551–4
[25] Preiss P, Sauerbrey R, Zubairy M S, Endrich R, Giese E, Kling P, Knobl M and Schleich W P 2012 *Proc. 34th Free-Electron Laser Conf.* (*Nara, Japan*) pp 93–6
Endrich R, Giese E, Kling P, Sauerbrey R and Schleich W P 2014 *Proc. 36th Free-Electron Laser Conf.* (*Basel, Switzerland*) pp 353–7
Kling P, Endrich R, Giese E, Sauerbrey R and Schleich W P 2014 *Proc. 36th Free-Electron Laser Conf.* (*Basel, Switzerland*) pp 348–52
[26] Bambini A and Renieri A 1978 *Lett. Nuovo Cimento* **21** 399–404
Bambini A, Renieri A and Stenholm S 1979 *Phys. Rev.* A **19** 2013–25
[27] Jaynes E T and Cummings F W 1963 *Proc. IEEE* **51** 89–109
[28] Schmüser P, Dohlus M and Rossbach J 2008 *Ultraviolet and Soft X-Ray Free-Electron Lasers* (Heidelberg: Springer)
[29] Meystre P and Sargent M 2007 *Elements of Quantum Optics* (Berlin: Springer)
[30] Sargent M, Scully M O and Lamb W E 1974 *Laser Physics* (Reading, MA: Addison-Wesley)
[31] Piovella N and Bonifacio R 2006 *Nucl. Instrum. Methods Phys. Res.* A **560** 240–4
[32] Martin P J, Oldaker B G, Miklich A H and Pritchard D E 1988 *Phys. Rev. Lett.* **60** 515–8
[33] Bragg W L 1912 *Proc. Camb. Phil. Soc.* **17** 43–57
[34] Giese E, Roura A, Tackmann G, Rasel E M and Schleich W P 2013 *Phys. Rev.* A **88** 053608
[35] Giltner D M, McGowan R W and Lee S A 1995 *Phys. Rev.* A **52** 3966–72
[36] Szigeti S S, Debs J E, Hope J J, Robins N P and Close J D 2012 *New J. Phys.* **14** 023009
[37] Bonifacio R, Casagrande F, Cerchioni G, de Salvo Souza L, Pierini P and Piovella N 1990 *Riv. Nuovo Cimento* **13** 1–69
[38] Bonifacio R, Piovella N and Cola M M M 2007 *Int. J. Mod. Phys.* A **22** 3776–83
[39] http://flash.desy.de/accelerator/ accessed 3rd June 2015
[40] Bonifacio R, Piovella N, Robb G R M and Cola M M 2005 *Opt. Commun.* **252** 381–96
[41] Bonifacio R 2005 *Nucl. Instrum. Methods Phys. Res.* A **546** 634–8
[42] Schlicher R R, Scully M O and Walther H 1987 Vorschlag für einen kompakten Freie-Elektronen Laser mit einem elektromagnetischen Undulator für den Infrarot und weichen Röntgenbereich *Technical Report* Max-Planck Institut für Quantenoptik
Gea-Banacloche J, Moore G T, Schlicher R R, Scully M O and Walther H 1987 *IEEE J. Quantum Electron.* **23** 1558–70
[43] Sprangle P, Hafizi B and Peñano J R 2009 *Phys. Rev. Spec. Top.—Accelerators Beams* **12** 050702
[44] Steiniger K, Bussmann M, Pausch R, Cowan T, Irman A, Jochmann A, Sauerbrey R, Schramm U and Debus A 2014 *J. Phys. B: At. Mol. Opt. Phys.* **47** 234011
[45] Jackson J D 1999 *Classical Electrodynamics* (New York: Wiley)
[46] Nayfeh A H 1973 *Perturbation Methods* (New York: Wiley)